

The relation between the ADF and the ionized nebular mass in PNe

Miriam Peña,¹* Francisco Ruiz-Escobedo¹ and Brenda N. Juárez Torres,²

¹ Universidad Nacional Autónoma de México, Instituto de Astronomía, Apdo. Postal 70264, 04510, Ciudad de México

² Universidad Nacional Autónoma de México, Facultad de Ciencias, Av. Universidad 3000, 04510, Ciudad de México

Accepted XXX. Received YYY; in original form ZZZ

ABSTRACT

In this work we analyze the proposed relation between ADFs and ionized masses in planetary nebulae. For this, we have collected from the literature the ADFs and other parameters such as heliocentric distances, H β luminosities, logarithmic reddening correction at H β , c(H β), electron densities and others and we calculated the ionized mass for a sample of 132 PNe, 27 of which possess a binary central star (14 are close binaries). In addition the distribution of these objects in the Galaxy is analyzed. The ionized masses were calculated considering two different electron densities, the one provided by the [S II] density sensitive lines ratio and the one provided by the [Cl III] lines ratio. No relation was found between ionized masses and ADFs for this sample, although it is confirmed than the PNe with the largest ADFs correspond in general to objects with a close binary central star, although it is important to say that about 20 percent of these objects have an ADF larger than 5 but smaller than 10. Therefore a PN having a close binary central star does not necessarily exhibit an extremely large ADF. We also have searched for possible relations between the ADFs and the stellar atmospheres, divided in H-rich and H-poor stars. No particular relation was found. Interestingly, several PNe with a [WR] H-poor CSPN present an ADF larger than 10, but so far they have not been reported as having a binary central star.

Key words: ISM: abundances - planetary nebulae: general - stars: AGB and post-AGB - binaries (including multiple): close

1 INTRODUCTION

A very important unresolved problem in the determination of chemical abundances of photo-ionized nebulae is the abundance discrepancy problem which appears when abundances are derived by using collisionally excited lines and recombination lines. It is parameterized by the so called Abundance Discrepancy Factor (ADF) which is defined as the ratio between the abundance derived from recombination lines (RLs) and that derived from collisionally excited lines (CELS). Usually it is measured for the O $^{+2}$ /H $^{+}$ abundance ratio.

$$ADF(O^{+2}) = N(O^{+2})_{RLs}/N(O^{+2})_{CELS}. \quad (1)$$

When available, the ADF has been derived for other ions such as C $^{+2}$, N $^{+}$ and Ne $^{+2}$. As ADF(O $^{+2}$) is the most commonly measured value in the literature we will use it, and henceforth it will be denoted simply as ADF throughout the text.

The abundance discrepancy problem occurs in H II regions and planetary nebulae (PNe) as well. It was first reported by Wyse (1942). In general, it has been found that ADF values are between 1.5 and 3 in H II regions (Peimbert et al. 2017) and they are larger in PNe, with values between 1.5 and 5, but values larger than 5 have been found in a number of PNe (Corradi et al. 2015; Peimbert et al. 2017). There are a few extreme cases where ADFs larger than several tens have been reported, such as the case of Abell 30 with an ADF of about 600 – 770 in its central filaments (Wesson et al. 2003), Abell 46 with an ADF of about 120 in its central region (Corradi et al. 2015), Abell 58

showing an ADF of 90 (Wesson et al. 2008) and Hf 2-2, with an ADF of 83 (Wesson et al. 2018).

Even ADF values as low as 2 imply a big problem in the chemistry of photo-ionized nebulae because it is not clear which are the real chemical abundances in the ionized medium and this has important repercussions in the analysis of several subjects such as the stellar evolution, the chemical evolution of galaxies and the Universe, etc.

Several solutions have been proposed to explain the ADF problem (see Espíritu & Peimbert 2021 for a complete list). The two most important solutions have been extensively analyzed. The first one is the possible presence of large temperature fluctuations in a chemically homogeneous plasma (Peimbert et al. 2017, and references therein); the fluctuations are larger than those predicted by photo-ionization models, and they have been used mainly to analyze ADFs in H II regions through the parameter t^2 that represents the size of the temperature fluctuations (Esteban et al. 2009 and Méndez-Delgado et al. 2023). The second solution corresponds to bi-abundance models where small H-deficient inclusions would be mixed with the H-rich hot plasma (Liu et al. 2000), these inclusions would be cold with T_e of about 1,000 K, and heavy element recombination lines would originate predominantly in this plasma. According to several authors (e. g., Espíritu & Peimbert 2021; Liu 2006; Peimbert & Peimbert 2013; Wesson et al. 2005) ADF values as large as 5 could be explained by the presence of temperature fluctuations in a chemically homogeneous plasma.

However, in several works the possibility of different plasmas of slightly different chemistry and physical conditions, coexisting in the nebulae, cannot be discarded. This possibility has been studied in the

* E-mail: miriam@astro.unam.mx

works by García-Rojas et al. (2016, 2022), Peña et al. (2017), Richer et al. (2013, 2019, 2022), Ruiz-Escobedo & Peña (2022), Espíritu & Peimbert (2021), and others, and can be studied through kinematic analysis or spatial distribution analysis.

A possible correlation between the ADF and the properties of PNe has been explored in some works of the literature (see, e. g., Wesson et al. 2018, and references therein). In the analysis of ADFs in several PNe, Corradi et al. (2015) and Wesson et al. (2018) found that ADF values seem to be associated to the binarity of the central stars, and in the case of close binary stars the ADFs tend to be large. Corradi et al. (2015) suggest that the ADF value might be related with the ionized mass of the PNe. In this work we aim to explore this suggestion, therefore, we collected data from the literature to derive the ionized masses of PNe and to search for a possible relation between these two parameters. We also explore the possible relation between ADFs and the stellar atmosphere.

This paper is organized as follows. In §2 the analyzed PNe sample is presented and its distribution in the Galaxy is studied. In §3 the ionized masses of PNe are calculated after determining the [S II] and [Cl III] electron densities. In §4 the ADF values and their possible relation with the central star atmosphere are presented. In §5 the possible relation between ADFs and the ionized mass is discussed. Our conclusions are presented in §6.

2 THE SAMPLE OF ANALYSED PNE

Our sample consists of 132 Galactic PNe from the list compiled by R. Wesson at <https://www.nebulosresearch.org/adfs/>, last updated on 9th January 2024. It is the largest compilation of PNe with determined values of ADF. We have also included the recent ADF values determined for IC 4663 (Mohery et al. 2023) and for M 3-27 (Ruiz-Escobedo et al. 2024) that have not yet been included in Wesson's compilation. In Table A1 we list the common names, PN G number, heliocentric distances D adopted from the work by Hernández-Juárez et al. (2024), central star binary, spectral classification of the central star as presented in the catalog by Weidmann et al. (2020), nebular diameters in arcsec, X_G , Y_G and Z_G coordinates (coordinates projected on the Galactic plane and height above the Galactic plane, measured relative to the Sun position), and the Galactocentric distance R_G . Binary central stars were taken from the compilation by Dr. D. Jones, available at <https://www.drdjones.net/bcspn/>, last updated on 15th September 2024 (Jones & Boffin 2017; Boffin & Jones 2019).

The values for X_G , Y_G and Z_G are given by:

$$X_G = D \cos l \cos b \quad (2)$$

$$Y_G = D \sin l \cos b \quad (3)$$

$$Z_G = D \sin b \quad (4)$$

where the origin of coordinates is the Sun position and l and b are the Galactic longitude and latitude, respectively.

The Galactocentric distance is derived from:

$$R_G = \sqrt{(X_G - X_{GC})^2 + (Y_G - Y_{GC})^2} \quad (5)$$

where $X_{GC} = 8$ kpc and $Y_{GC} = 0$ kpc are the coordinates of the Galactic centre (Stanghellini & Haywood 2010).

The Galactic position of the objects in the sample is shown in Fig. 1 where PNe with a close binary central star¹ are shown as blue diamonds. As expected, the PNe are close to the Galactic plane and

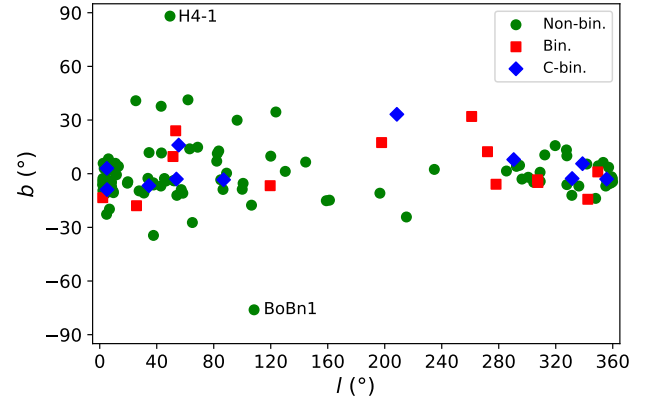


Figure 1. The Galactic distribution of the PNe (l , b) in the sample is shown. PNe with distant binary central stars are shown as red squares, PNe with close binary central star are shown as blue diamonds and PNe without a binary central star are shown as green dots. A couple of PN in the galactic halo are marked.

more concentrated towards the Galactic centre (Acker et al. 1992). A couple of PNe located in the Galactic halo are marked.

In Fig. 2 the (X_G, Y_G) distribution of the PNe of the sample is shown. Most of the PNe have X_G and Y_G values lower than 10 kpc. In this figure, the two objects at largest distances are Hen 2-436, which belongs to the Sagittarius spheroidal galaxy (Zijlstra & Walsh 1996), and Sp 4-1, which is a halo PN.

The distribution in Z_G is presented in Fig. 3 where it is verified that most of the PNe are very close to the Galactic plane except those objects identified as belonging to the Galactic halo.

In these figures it is observed that PNe with a binary central star are in the region $-3.7 \text{ kpc} \leq X_G \leq 8.8 \text{ kpc}$ and $-2.6 \text{ kpc} \leq Y_G \leq 5.3 \text{ kpc}$, while PNe without a reported binary central star are distributed in a larger zone, $-4.4 \text{ kpc} \leq X_G \leq 15 \text{ kpc}$ (Hen 2-436 is not considered) and $-10 \text{ kpc} \leq Y_G \leq 10 \text{ kpc}$ (without considering Sp 4-1). This would be indicating that PNe with a binary star are located nearer the solar vicinity. It is possible that a selection effect is perturbing this graph, because some PNe marked as "not having a binary central star" (shown in green) could possess one not discovered so far.

In Fig. 3, showing the distribution of the sample relative to the Galactic plane, it is observed that most of the objects are very near the Galactic plane, except those belonging to the Galactic halo: H 4-1, DdDm 1, Sp 4-1 and BoBn 1. PNe with a binary central star seem more concentrated but, again, this could be due to a selection effect.

3 THE IONIZED MASS

Corradi et al. (2015) discussed a procedure to calculate the ionized mass of Abell 46, Abell 66 and Ou 5 by assuming that there exist two different plasmas in the nebula, a hot, one with low metallicity and emitting mainly the CELs, and a cooler one, with high metallicity and emitting mainly the RLs. The procedure is based on the total flux of $H\beta$, the distance, the electron density and the temperature of the gas determined from CELs and RLs. They concluded that the majority of the H is in the hot gas component and the $H\beta$ emission is mainly

¹ A close binary star is defined as a binary where the rotation period is \leq

1.15 days (Wesson et al. 2018). The periods were obtained from <https://www.drdjones.net/bcspn/>.

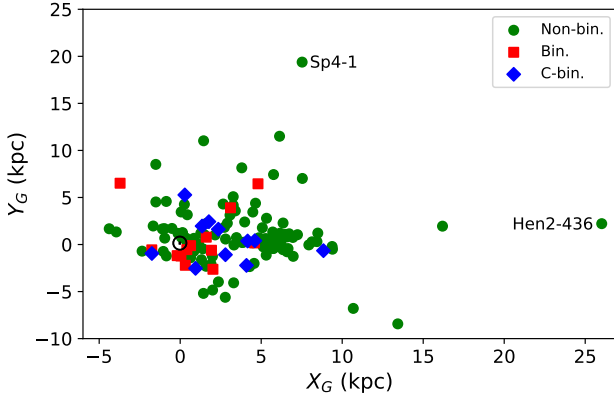


Figure 2. The (X_G, Y_G) distribution of the PNe of the sample is shown. Symbols and colours are the same as in Fig. 1. \odot represents the solar position.

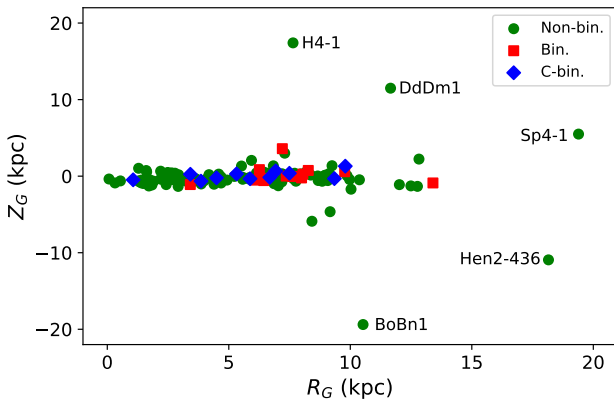


Figure 3. The Galactic distribution of PNe in the sample, relative to the Galactic plane, is shown. Most of the objects are very close to the Galactic plane. Several PNe of the Galactic halo are marked. Symbols and colours are the same as in Fig. 1.

produced in the low metallicity zone where the temperature is given by the $[\text{O III}]$ lines while the high metallicity zone (with abundances given by RLs) contains a small amount of H and it emits a small amount of $H\beta$. Therefore, following this conclusion, we calculate the ionized mass by assuming that most of the H resides in the hot component and that the nebular ionized mass can be calculated following the expression by Stasińska et al. (2013):

$$M_{ion} = \frac{37.5 \times L_{H\beta}}{n_e} \quad (6)$$

where M_{ion} is the ionized mass in solar units, $L_{H\beta}$ is the total de-reddened luminosity in $H\beta$ in solar units, and n_e is the electron density in particles per cm^3 . Eq. 6 is equivalent to the expression given by Corradi et al. (2015) and in our case it has been assumed that the electron temperature is 10^4 K which represents a good average of the T_e ([O III]) for PNe (see e.g., Henry et al. 2004).

The electron density can be determined with different density sensitive line ratios, being the more used $[\text{S II}]\lambda\lambda 6731/6717$, $[\text{O II}]\lambda\lambda 3729/3726$ and $[\text{Cl III}]\lambda\lambda 5537/5517$. We have compiled from the literature the density sensitive line ratios of [S II] and [Cl III] which

Table 1. Atomic data used for n_e calculations.

Ion	Transition probabilities	Collisional strength
S^+	Podobedova et al. (2009)	Tayal & Zatsarinsky (2010)
Cl^{+2}	Mendoza (1983)	Butler & Zeippen (1989)

are more easily available than the $[\text{O II}]$ lines, that are in the ultraviolet and separated by only 2 Å. Thus, electron densities were calculated from $[\text{S II}]$ and $[\text{Cl III}]$ lines in a homogeneous way by assuming in all cases a $T_e = 10^4$ K and by using the routine *get.TemDen* from PyNEB (Luridiana et al. 2015), version 1.1.18, and the atomic data listed in Table 1. The derived values are listed in Table A2 where we also included the references for the adopted line ratios. These density values were used to derive ionized masses according to Eq. 6.

The luminosity $L(H\beta)$ can be derived from the measured flux at $H\beta$ (corrected for reddening using the logarithmic extinction coefficient value, $c(H\beta)$, listed in column 2 of Table A3), and the distance D through the next expression:

$$L(H\beta) = 4\pi D^2 F(H\beta) \quad (7)$$

To estimate the total $L(H\beta)$ we need to consider if the value of the flux $F(H\beta)$ found in the literature is global (including all the nebula) or measured through a slit, usually smaller than the nebular size. In Table A3 we present the $H\beta$ fluxes (from slit and global) obtained from the literature, and the luminosities derived from them.

In Table A4 the derived ionized masses are presented. In different columns it is established if the mass was derived from the total $L(H\beta)$ or from a partial value obtained from a slit measurement. To search for the relation between ADFs and ionized masses, only the masses derived from the total $L(H\beta)$ were considered due to the masses derived from slit data are usually not including the complete nebula.

4 THE VALUES OF ADF

As it was said in §2, the values of ADF for the PNe sample were directly obtained from the compilation by R. Wesson², complemented with the two ADF values taken from the works by Mohery et al. (2023); Ruiz-Escobedo et al. (2024), and are listed in Table A4. They correspond to ADFs calculated by different authors (references presented in the same table), according to the Eq. 1 given in the Introduction. A histogram with the ADF values is shown in Fig. 4. In this figure it is observed that the ADF values for PNe without a reported binary central star (shown in blue) are between 2 and 6, except for two objects with ADF of about 40. On the other hand, the values for PNe with a reported binary central star are distributed in a wider rank, up to a value of 770. In the zone of $\log \text{ADF}$ larger than 1.0 all the objects, except two, correspond to PNe with a binary central star. As a matter of fact, for the 11 PNe with close binary central star shown in Fig. 6, it is found that all of them have ADF value larger than 5, and only 3 objects of this sample present an ADF smaller than 10. It is interesting to notice that an important fraction of PNe with a binary star does not present a extremely large ADF.

² <https://www.nebulosresearch.org/adfs/>

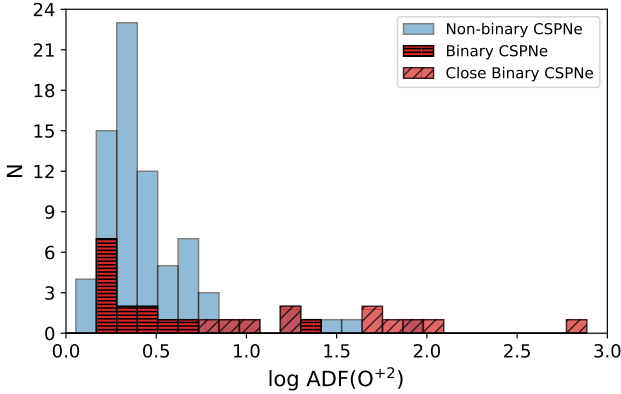


Figure 4. The distribution of ADF values. In blue we show the regular PNe and in red, the PNe with a binary central star or a close binary central star.

4.1 The ADF and the central star atmosphere

The spectral analysis of central stars (CSPNe) shows that the stellar atmospheres could be classified as H-rich or H-poor. Among the latter ones we find [WR] stars, PG 1159 stars and some H-poor white dwarfs. In the works by García-Rojas et al. (2009, 2013) 15 PNe with a [WR] central star (hence a H-poor central star) were analyzed finding that these objects have low to normal ADF. This is even the case of NGC 5189, which was lately reported as having a binary central star with a period of 4 days (Manick et al. 2015). In this section, we extend the works by García-Rojas et al. (2009, 2013) by analyzing more than a hundred objects possessing different types of central stars: 48 H-rich and 32 H-poor, which include [WR], PG 1159 and other H-poor type stars.

In order to search for possible relations between the ADFs and the central star atmosphere, we use the spectral classification given in the catalog by Weidmann et al. (2020), listed in Table A1. From our original sample of 132 PNe, only 103 PNe possess a classified CSPN in the list by Weidmann et al. (2020). In this catalog, occasionally only the primary star is classified in binary stars and the secondary appears with a quotation mark.

In Fig. 5 the distribution of ADFs grouped by the central star atmosphere is shown. Binary central stars (distant and close) are indicated with different symbols. The upper panel presents the H-rich CSPNe (48 objects distributed in 29 non-binary stars, 9 binaries and 10 close binaries). It is clear that the PNe with ADFs larger than 5 have close binary stars. In the middle panel the objects with H-poor CSPNe (32 objects distributed in 27 non-binary stars, 4 binaries and 1 close binary) show a distribution more concentrated towards lower ADFs although there are five objects with ADF larger than 10 of which only Abell 30, appearing to the right with an ADF = 770 measured in its central knots, has been identified as having a close binary star. It is tempting to suggest that the other 4 objects which are Abell 58, IC 4663, NGC 1501, and NGC 40, all of which have a [WR] star, could possess also a close binary central star. In the lower panel with not classified central stars there are 23 objects distributed in 21 non-binary stars, 1 binary and 1 close binary. PNe included in this group are objects with central stars reported as *wels*, *cont*, and *EL* CSPNe in the list by Weidmann et al. (2020). These objects present a distribution similar to the upper panel and the only object with a close binary star is NGC 6337 that possesses an ADF of 18.

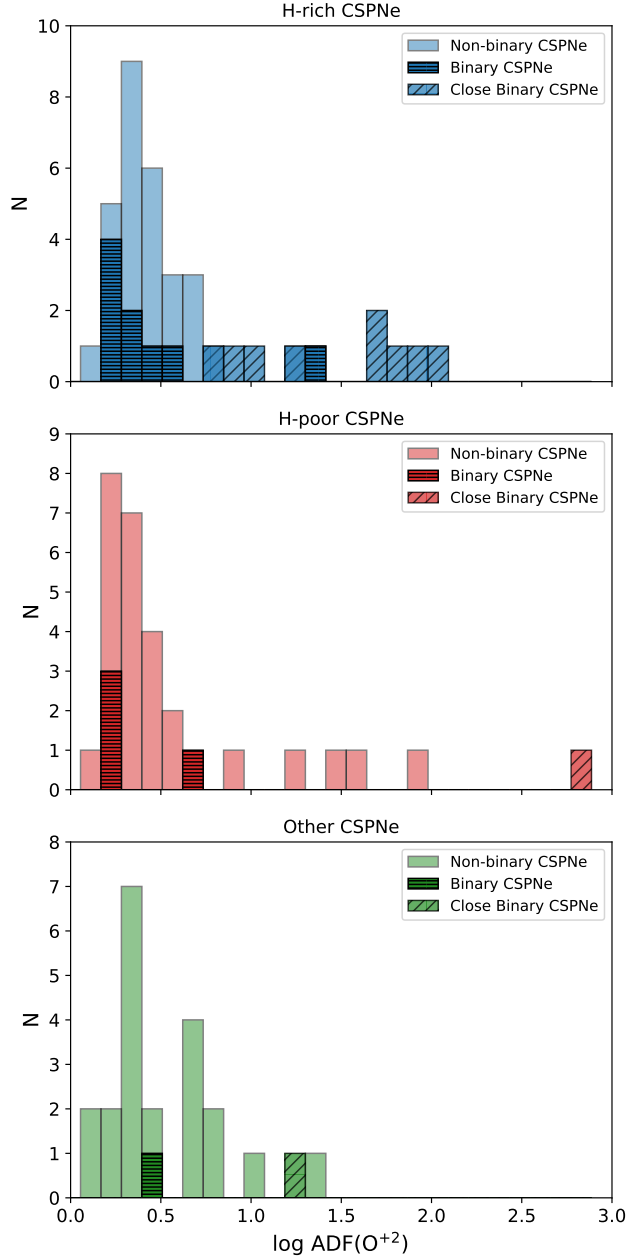


Figure 5. The distribution of ADF values grouped by the type of central star atmosphere. In blue the H-rich CSPNe are shown, in red the H-poor CSPNe are indicated, and in green, the other classification by Weidmann et al. (2020) are pointed out.

NGC 6337 is next to M 1-42, a non-binary object with an ADF of 20. It is possible that M 1-42 has a not-reported binary central star.

5 THE ADFS AND THE NEBULAR IONIZED MASSES

Fig. 6 shows the relation between the ADF values and the ionized mass derived as described in §3 by using our computed [S II] electron densities, and the global luminosity of H β . No obvious relation between these two parameters is found, although it is evident that several PNe with a close binary central star have the largest ADFs

M_{ion}	Data number	R_s	P_v
[S II] Slit	96	0.0300	0.7713
[Cl III] Slit	77	0.1928	0.0929
[S II] Global	116	0.0384	0.6810
[Cl III] Global	90	0.1062	0.3189

Table 2. Results from the Spearman statistical test showing the relation between ionized masses and the ADFs.

(in agreement with the results presented previously by Corradi et al. 2015 and other authors). There are also many PNe with a binary star (distant) which present a much smaller ADF as it is also evident in Fig. 5. The PNe with no binary star are distributed all over the diagram. The same is found when the [Cl III] density is used, as it is shown in Fig. 7 where no evident relation between ADFs and ionized masses is found. Unfortunately, there is only one close binary central star object (Hf 2-2) in this diagram with [Cl III] density determined and showing a large ADF.

To check better that there is no relation between these parameters, we run a statistical test. The Spearman correlation coefficient was used. The results are presented in Table 2 where the R_s and P_v values are listed. Both values indicate no correlation between the parameters.

In relation to the ionized mass of the objects, in Figs. 6 and 7 it is clearly observed that PNe with close binary central stars have all type of masses with $\log M_{ion}$ from -2 to almost 0 (in solar masses). In this sense, PNe with close binary stars behave equal to PNe with not binary star reported. The PNe with the lowest ionized masses in our sample are Hen 2-86, that has a $M_{ion}[\text{S II}] \sim 6 \times 10^{-3} M_\odot$, and Vy 2-2, that has a $M_{ion}[\text{Cl III}] \sim 3.4 \times 10^{-3} M_\odot$. They have not a binary central star, and have reported ADFs of 1.9 and 4.3 , respectively.

Santander-García et al. (2022) calculated the ionized and molecular masses of 21 post-common envelope (post-CE) PNe with close binary central star. The molecular masses could be determined only in a couple of objects. They concluded that post-CE PNe arising from single degenerate (SD) systems are as massive as their single-star "regular" counterparts, with a geometrical average value of $0.15 M_\odot$ while post-CE PNe arising from double degenerate (DD) systems³ are considerably more massive than SD systems and "regular" PNe, with a geometrical average mass of $0.31 M_\odot$. Therefore from the work by Santander-García et al. it is evident that the masses of post-CE PNe are not particularly low and they behave equal to PNe with not binary star.

6 CONCLUSIONS

In this work, data for 132 PNe with known ADF value were compiled including their heliocentric distances, galactic coordinates, H β fluxes, logarithmic extinction coefficients, c(H β), spectral types of the central stars (available for 103 objects), and nebular sizes. Twenty seven PNe of the sample have been identified as having a binary central star, fourteen of which are close binary central stars. The electron densities were derived by us in a homogeneous way from [S II] and [Cl III] density sensitive lines ratios obtained from the literature and using routines from PyNEB.

³ According to Santander-García et al. (2022), SD are binary systems where one of their components is a post-asymptotic giant branch (post-AGB) star while DD are binary systems where both components are post-AGB stars.

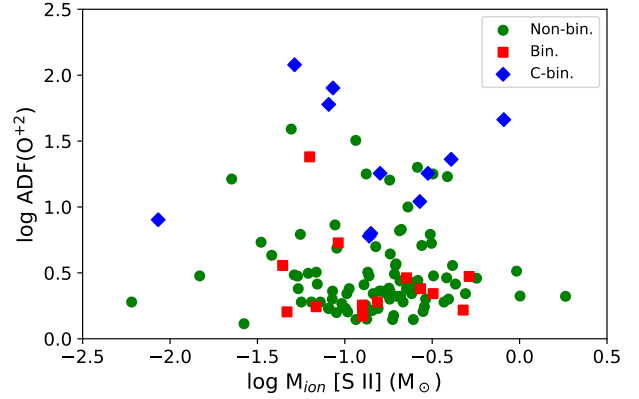


Figure 6. Relation between the ionized masses (derived from the [S II] densities and the global H β luminosities) vs. the ADFs. PNe with distant binary central stars are shown as red squares, PNe with close binary central stars are shown as blue diamonds and PNe without a binary central stars are shown as green dots.

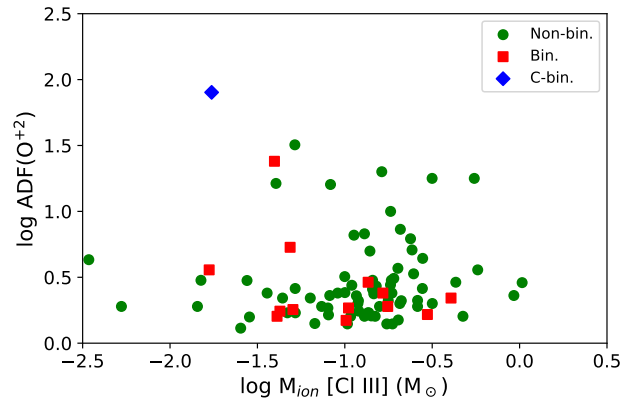


Figure 7. Relation between the ionized masses (derived from the [Cl III] densities and the global H β luminosities) vs. the ADFs. Symbols and colors are the same as in Fig. 6.

Considering their galactic coordinates, we analyzed the distribution of these objects in the Galaxy calculating their (X_G , Y_G , Z_G) positions, with the Sun at the origin of coordinates and the Galactic centre at 8 kpc in the X direction. From the X_G position of the objects, we found that most of them are in the direction towards the Galactic centre with values of X_G in the range from -5 kpc (anti-centre direction) to 10 kpc. Regarding the distribution in Y_G , most of the objects are within -10 and 10 kpc. The distribution of Z_G values (height above the Galactic plane) shows that most of the objects are near the Galactic plane, having a Z_G value within -3 and 3 kpc with exception of the halo PNe which have larger Z_G . The distribution of our objects in the Galaxy is similar to the Galactic distribution of larger samples of PNe (see e.g., Acker et al. 1992).

In §4.1 we have analyzed the possible relation between the ADFs and the stellar type atmospheres. Although one might expect that H-poor central stars can produce nebulae with large ADFs if H-poor material is ejected from the H-poor star, no differences are found in the ADF values for PNe with H-rich and H-poor central stars. In

both cases most PNe with large ADFs are those with close binary central stars. Due to this, we are suggesting that Abell 58, IC 4663, NGC 1501, and NGC 40, all of which have a [WC] central star and an ADF larger than 20, might possess a close binary central star.

The main aim of this work was to verify the suggestion by Corradi et al. (2015) about a possible relation between the ADF values and the ionized masses of PNe. Corradi et al. (2015) calculated the ionized masses of three PNe with large ADF values and a close binary star (Abell 43, Abell 65 and Ou 5) which together with results for Hf 2-2 by Liu et al. (2006), led them to the conclusion that PNe with large ADF have low ionized masses. We calculated the ionized masses of a large number of PNe, using the electron densities derived from [S II] and [Cl III] density sensitive line ratios, and by assuming that the electron temperature is 10^4 K and $H\beta$ luminosity is mainly emitted in the low metallicity zone where the CELs are produced. No attempt was made to calculate the possible contribution to $H\beta$ in the zone where the RLs are mainly produced (a procedure performed by Corradi et al. 2015 and more recently by García-Rojas et al. 2022) due to it is not expected that the H-poor zone emits an important amount of H recombination lines.

No relation was found between the ADFs and the ionized masses, whether visually in the figures or by means of a statistical test (Spearman coefficient). The ionized masses cover a range of $\log M_{ion}$ between -2 and 0, in solar masses. It should be noticed that PNe with close binary central star (blue diamonds in Fig. 6) have ionized masses in all this range and the same happens for objects with not binary star. Santander-García et al. (2022) derived a similar result for 21 post-CE PNe. It is important to note that about 20 percent of the PNe in our sample, with a detected close binary star, have an ADF value in the 5 to 10 range, therefore a PN having a close binary central star does not necessarily exhibits an extremely large ADF.

The origin of the ADF in PNe is still an open problem although attempts to correlate it with temperature fluctuations or small H-poor inclusions in the nebulae have been made. Temperature fluctuations seem to work in the case of H II regions (Méndez-Delgado et al. 2023) where the ADFs are lower than 3 but, as mentioned in the Introduction, such a mechanism can not explain ADFs larger than 5.

It has been suggested for some time that there might be different plasmas with different physical conditions and different chemistry coexisting in the nebula and that could be causing the ADFs. The three objects analyzed by Corradi et al. (2015) show such different plasmas with an inner one H-poor and richer in heavy elements and an outer one H-rich and with low metallicity. Also such different plasmas have been found in other PNe, such as the case of NGC 6778, M 1-42, Hf 2-2 and others (García-Rojas et al. 2016, 2022). In addition, different plasmas with different kinematics have been found in some PNe, one emitting mainly the CELs and the other emitting mainly the RLs (Peña et al. 2017; Richer et al. 2013, 2022). When two or more plasma components with different physical conditions are present in the ionized gas of a PN, the relevance of an ADF determination becomes less obvious.

Undoubtedly, much more work is required to disentangle the origin of large ADFs in PNe.

ACKNOWLEDGEMENTS

We are deeply grateful to Diego B. Hernández-Juárez who helped us with the statistical probes and for providing distance data previous to publication. We thank an anonymous referee whose useful comments helped to improve this article. This work received partial financial support from the grant IN 111423, DGAPA, UNAM.

DATA AVAILABILITY

The data underlying this article will be shared on reasonable request to the corresponding author.

REFERENCES

- Acker A., Stenholm B., Tylenda R., Raytchev B., 1991, *A&AS*, **90**, 89
Acker A., Marcout J., Ochsenbein F., Stenholm B., Tylenda R., Schohn C., 1992, The Strasbourg-ESO Catalogue of Galactic Planetary Nebulae. Parts I. European Southern Observatory.
Barker T., 1978, *ApJ*, **219**, 914
Boffin H. M. J., Jones D., 2019, The Importance of Binaries in the Formation and Evolution of Planetary Nebulae, doi:10.1007/978-3-030-25059-1.
Bojičić I. S., Filipović M. D., Urošević D., Parker Q. A., Galvin T. J., 2021, *MNRAS*, **503**, 2887
Butler K., Zeippen C. J., 1989, *A&A*, **208**, 337
Cahn J. H., Kaler J. B., 1971, *ApJS*, **22**, 319
Cahn J. H., Kaler J. B., Stanghellini L., 1992, *A&AS*, **94**, 399
Chu Y.-H., Jacoby G. H., Arendt R., 1987, *ApJS*, **64**, 529
Clegg R. E. S., Peimbert M., Torres-Peimbert S., 1987, *MNRAS*, **224**, 761
Collins G. W. I., Daub C. T., O'Dell C. R., 1961, *ApJ*, **133**, 471
Corradi R. L. M., García-Rojas J., Jones D., Rodríguez-Gil P., 2015, *ApJ*, **803**, 99
Ercolano B., Wesson R., Zhang Y., Barlow M. J., De Marco O., Rauch T., Liu X. W., 2004, *MNRAS*, **354**, 558
Espíritu J. N., Peimbert A., 2021, *MNRAS*, **508**, 2668
Esteban C., Bresolin F., Peimbert M., García-Rojas J., Peimbert A., Mesa-Delgado A., 2009, *ApJ*, **700**, 654
Fang X., Liu X. W., 2011, *MNRAS*, **415**, 181
García-Rojas J., Peña M., Peimbert A., 2009, *A&A*, **496**, 139
García-Rojas J., Peña M., Morisset C., Mesa-Delgado A., Ruiz M. T., 2012, *A&A*, **538**, A54
García-Rojas J., Peña M., Morisset C., Delgado-Ingla G., Mesa-Delgado A., Ruiz M. T., 2013, *A&A*, **558**, A122
García-Rojas J., Madonna S., Luridiana V., Sterling N. C., Morisset C., Delgado-Ingla G., Toribio San Cipriano L., 2015, *MNRAS*, **452**, 2606
García-Rojas J., Corradi R. L. M., Monteiro H., Jones D., Rodríguez-Gil P., Cabrera-Lavers A., 2016, *ApJ*, **824**, L27
García-Rojas J., Delgado-Ingla G., García-Hernández D. A., Dell'Agli F., Lugaro M., Karakas A. I., Rodríguez M., 2018, *MNRAS*, **473**, 4476
García-Rojas J., Morisset C., Jones D., Wesson R., Boffin H. M. J., Monteiro H., Corradi R. L. M., Rodríguez-Gil P., 2022, *MNRAS*, **510**, 5444
Garnett D. R., Dinerstein H. L., 2001, *ApJ*, **558**, 145
Hawley S. A., Miller J. S., 1978, *ApJ*, **220**, 609
Henry R. B. C., Kwinter K. B., Balick B., 2004, *AJ*, **127**, 2284
Henry R. B. C., Kwinter K. B., Dufour R. J., Skinner J. N., 2008, *ApJ*, **680**, 1162
Hernández-Juárez D., Rodríguez M., Peña M., 2024, *RevMexAA*, **60**, 227
Jones D., Boffin H. M. J., 2017, *Nature Astronomy*, **1**, 0117
Jones D., Boffin H. M. J., Rodríguez-Gil P., Wesson R., Corradi R. L. M., Miszalski B., Mohamed S., 2015, *A&A*, **580**, A19
Jones D., Wesson R., García-Rojas J., Corradi R. L. M., Boffin H. M. J., 2016, *MNRAS*, **455**, 3263
Kaler J. B., 1976, *ApJ*, **210**, 113
Kaler J. B., 1978, *ApJ*, **226**, 947
Kaler J. B., 1980, *ApJ*, **239**, 78
Kaler J. B., 1983, *ApJ*, **271**, 188
Kaler J. B., Lutz J. H., 1985, *PASP*, **97**, 700
Kapusta J. I., Olive K. A., 1990, *Phys. Rev. Lett.*, **64**, 13
Kohoutek L., Martin W., 1981, *A&AS*, **44**, 325
Liller W., 1955, *ApJ*, **122**, 240
Liu X.-W., 2006, in Barlow M. J., Méndez R. H., eds, IAU Symposium Vol. 234, Planetary Nebulae in our Galaxy and Beyond. pp 219–226 (arXiv:astro-ph/0605082), doi:10.1017/S1743921306003000
Liu X. W., Storey P. J., Barlow M. J., Clegg R. E. S., 1995, *MNRAS*, **272**, 369

- Liu X. W., Storey P. J., Barlow M. J., Danziger I. J., Cohen M., Bryce M., 2000, *MNRAS*, **312**, 585
- Liu X. W., Luo S. G., Barlow M. J., Danziger I. J., Storey P. J., 2001, *MNRAS*, **327**, 141
- Liu Y., Liu X. W., Luo S. G., Barlow M. J., 2004a, *MNRAS*, **353**, 1231
- Liu Y., Liu X. W., Barlow M. J., Luo S. G., 2004b, *MNRAS*, **353**, 1251
- Liu X. W., Barlow M. J., Zhang Y., Bastin R. J., Storey P. J., 2006, *MNRAS*, **368**, 1959
- Luridiana V., Morisset C., Shaw R. A., 2015, *A&A*, **573**, A42
- Madonna S., García-Rojas J., Sterling N. C., Delgado-Inglada G., Mesa-Delgado A., Luridiana V., Roederer I. U., Mashburn A. L., 2017, *MNRAS*, **471**, 1341
- Manick R., Miszalski B., McBride V., 2015, *MNRAS*, **448**, 1789
- McNabb I. A., Fang X., Liu X. W., 2016, *MNRAS*, **461**, 2818
- Méndez-Delgado J. E., Esteban C., García-Rojas J., Kreckel K., Peimbert M., 2023, *Nature*, **618**, 249
- Mendoza C., 1983, in Aller L. H., ed., IAU Symposium Vol. 103, Planetary Nebulae. pp 143–172
- Miszalski B., Manick R., Rauch T., Ilkiewicz K., Van Winckel H., Mikołajewska J., 2019, *Publ. Astron. Soc. Australia*, **36**, e042
- Mohery M., Ali A., Khames A. A., Snaid S., Mindil A., 2023, *Frontiers in Astronomy and Space Sciences*, **10**, 1322980
- Moreno H., Lasker B. M., Gutierrez-Moreno A., Torres C., 1988, *PASP*, **100**, 604
- O'Dell C. R., 1963, *ApJ*, **138**, 293
- Otsuka M., 2015, *MNRAS*, **452**, 4070
- Otsuka M., Tajitsu A., 2013, *ApJ*, **778**, 146
- Otsuka M., Hyung S., Lee S.-J., Izumiura H., Tajitsu A., 2009, *ApJ*, **705**, 509
- Otsuka M., Tajitsu A., Hyung S., Izumiura H., 2010, *ApJ*, **723**, 658
- Otsuka M., Meixner M., Riebel D., Hyung S., Tajitsu A., Izumiura H., 2011, *ApJ*, **729**, 39
- Otsuka M., Hyung S., Tajitsu A., 2015, *ApJS*, **217**, 22
- Otsuka M., Parthasarathy M., Tajitsu A., Hubrig S., 2017, *ApJ*, **838**, 71
- Peña M., Ruiz-Escobedo F., Rechy-García J. S., García-Rojas J., 2017, *MNRAS*, **472**, 1182
- Peña M., Parthasarathy M., Ruiz-Escobedo F., Manick R., 2022, *MNRAS*, **515**, 1459
- Peimbert A., Peimbert M., 2013, *ApJ*, **778**, 89
- Peimbert M., Peimbert A., Delgado-Inglada G., 2017, *PASP*, **129**, 082001
- Perek L., 1971, Bulletin of the Astronomical Institutes of Czechoslovakia, **22**, 103
- Perek L., Kohoutek L., 1967, Catalogue of Galactic Planetary Nebulae. Czechoslovak Academy of Sciences
- Podobedova L. I., Kelleher D. E., Wiese W. L., 2009, *Journal of Physical and Chemical Reference Data*, **38**, 171
- Richer M. G., Georgiev L., Arrieta A., Torres-Peimbert S., 2013, *ApJ*, **773**, 133
- Richer M. G., Guillén Tavera J. E., Arrieta A., Torres-Peimbert S., 2019, *ApJ*, **870**, 42
- Richer M. G., Arrieta A., Arias L., Castañeda-Carlos L., Torres-Peimbert S., López J. A., Galindo A., 2022, *AJ*, **164**, 243
- Robertson-Tessi M., Garnett D. R., 2005, *ApJS*, **157**, 371
- Ruiz-Escobedo F., Peña M., 2022, *MNRAS*, **510**, 5984
- Ruiz-Escobedo F., Peña M., Beltrán-Sánchez A. V., 2024, *MNRAS*, **528**, 4228
- Ruiz M. T., Peimbert A., Peimbert M., Esteban C., 2003, *ApJ*, **595**, 247
- Santander-García M., Jones D., Alcolea J., Bujarrabal V., Wesson R., 2022, *A&A*, **658**, A17
- Sharpee B., Baldwin J. A., Williams R., 2004, *ApJ*, **615**, 323
- Shaw R. A., Kaler J. B., 1982, *ApJ*, **261**, 510
- Shaw R. A., Kaler J. B., 1985, *ApJ*, **295**, 537
- Shaw R. A., Kaler J. B., 1989, *ApJS*, **69**, 495
- Simpson J., Jones D., Wesson R., García-Rojas J., 2022, *Research Notes of the American Astronomical Society*, **6**, 4
- Sowicka P., Jones D., Corradi R. L. M., Wesson R., García-Rojas J., Santander-García M., Boffin H. M. J., Rodríguez-Gil P., 2017, *MNRAS*, **471**, 3529
- Stanghellini L., Haywood M., 2010, *ApJ*, **714**, 1096
- Stasińska G., Peña M., Bresolin F., Tsamis Y. G., 2013, *A&A*, **552**, A12
- Tayal S. S., Zatsarinsky O., 2010, *ApJS*, **188**, 32
- Tsamis Y. G., Barlow M. J., Liu X. W., Danziger I. J., Storey P. J., 2003, *MNRAS*, **345**, 186
- Tsamis Y. G., Barlow M. J., Liu X. W., Storey P. J., Danziger I. J., 2004, *MNRAS*, **353**, 953
- Viadana L., de Freitas Pacheco J. A., 1985, *Revista Brasileira de Física*, **15**, 70
- Wang W., Liu X. W., 2007, *MNRAS*, **381**, 669
- Webster B. L., 1969, *MNRAS*, **143**, 79
- Webster B. L., 1983, *PASP*, **95**, 610
- Weidmann W. A., et al., 2020, *A&A*, **640**, A10
- Wesson R., 2024, A compilation of abundance discrepancy factors, rogers astronomy pages, <https://nebulousresearch.org/adfs/>
- Wesson R., Liu X. W., 2004, *MNRAS*, **351**, 1026
- Wesson R., Liu X. W., Barlow M. J., 2003, *MNRAS*, **340**, 253
- Wesson R., Liu X. W., Barlow M. J., 2005, *MNRAS*, **362**, 424
- Wesson R., Barlow M. J., Liu X. W., Storey P. J., Ercolano B., De Marco O., 2008, *MNRAS*, **383**, 1639
- Wesson R., Jones D., García-Rojas J., Boffin H. M. J., Corradi R. L. M., 2018, *MNRAS*, **480**, 4589
- Wyse A. B., 1942, *ApJ*, **95**, 356
- Zhang Y., Liu X. W., 2003, *A&A*, **404**, 545
- Zhang Y., Liu X. W., Luo S. G., Péquignot D., Barlow M. J., 2005, *A&A*, **442**, 249
- Zhang Y., Fang X., Chau W., Hsia C. H., Liu X. W., Kwok S., Koning N., 2012, *ApJ*, **754**, 28
- Zijlstra A. A., Walsh J. R., 1996, *A&A*, **312**, L21

Table A1: Galactic coordinates, PN G number, heliocentric distance (kpc), binarity (Close-binary, Binary, Non-binary), stellar classification, and diameter of PNe.

Name	PN G	Distance (kpc)	Binarity	CSPN	Diameter (arcsec)	Diam. ref.	X _G (kpc)	Y _G (kpc)	Z _G (kpc)	R _G (kpc)
Abell 30	208.5+33.2	2.38	C-bin.	[WC]-PG 1159 + ?	127.00	CK71	-1.748	-0.951	1.306	9.794
Abell 46	055.4+16.0	2.48	C-bin.	O(H)3 + ?	63.00	Cor15	1.353	1.962	0.685	6.930
Abell 58	037.6-05.1	5.68	Non-bin.	[WC 4-7]	44.00	Wes08	4.482	3.452	-0.511	4.928
Abell 63	053.8-03.0	3.01	C-bin.	sdO + ?	44.90	Cor15	1.771	2.428	-0.159	6.685
BoBn 1	108.3-76.1	19.96	Non-bin.	—	2.20	Ots10	-1.503	4.525	-19.382	10.525
Cn 1-5	002.2-09.4	4.56	Non-bin.	[WO 4]pec	7.00	WL07	4.494	0.180	-0.751	3.510
Cn 2-1	356.2-04.4	6.69	Non-bin.	Of	2.40	WL07	6.656	-0.432	-0.514	1.411
DdDm 1	061.9+41.3	17.38	Non-bin.	O(H)	0.60	CPT87	6.133	11.506	11.491	11.657
Fg 1	290.5+07.9	2.73	C-bin.	O(H)3-4 + ?	16.00	CKS92	0.947	-2.533	0.376	7.494
H 1-35	355.7-03.4	5.74	Non-bin.	wels?	2.00	WL07	5.714	-0.427	-0.347	2.326
H 1-40	359.7-02.6	7.95	Non-bin.	—	3.80	Mor88	7.941	-0.04	-0.373	0.071
H 1-41	356.7-04.8	5.37	Non-bin.	wels	9.60	WL07	5.343	-0.302	-0.449	2.675
H 1-42	357.2-04.5	5.15	Non-bin.	wels	5.80	WL07	5.128	-0.245	-0.408	2.882
H 1-50	358.7-05.2	9.42	Non-bin.	—	10.00	PK67	9.378	-0.21	-0.867	1.394
H 1-54	002.1-04.2	8.47	Non-bin.	—	4.80	WL07	8.442	0.311	-0.62	0.540
H 4-1	049.3+88.1	17.42	Non-bin.	—	2.70	KM81	0.369	0.429	17.411	7.643
Hb 4	003.1+02.9	3.83	Non-bin.	[WO 3]	6.20	PK67	3.819	0.212	0.195	4.186
Hen 2-73	296.3-03.0	6.27	Non-bin.	—	3.30	Wepg	2.783	-5.609	-0.336	7.660
Hen 2-86	300.7-02.0	4.62	Non-bin.	[WC 5-6]	5.60	CK71	2.358	-3.969	-0.168	6.899
Hen 2-96	309.0+00.8	5.24	Non-bin.	—	4.00	CK71	3.299	-4.071	0.081	6.219
Hen 2-118	327.5+13.3	13.01	Non-bin.	—	5.00	PK67	10.685	-6.789	3.000	7.301
Hen 2-155	338.8+05.6	3.01	C-bin.	O(H)3-5 + ?	14.50	CKS92	2.793	-1.083	0.298	5.319
Hen 2-158	327.8-06.1	15.95	Non-bin.	—	2.00	CK71	13.431	-8.432	-1.703	10.030
Hen 2-161	331.5-02.7	4.66	C-bin.	O(H)3-4 + ?	10.00	CKS92	4.092	-2.218	-0.226	4.494
Hen 2-283	355.7-03.0	8.88	C-bin.	—	5.00	Wepg	8.843	-0.651	-0.479	1.065
Hen 2-436	004.8-22.7	28.31	Non-bin.	—	10.00	PK67	26.019	2.217	-10.934	18.155
Hen 3-1357	331.3-12.1	5.00	Non-bin.	H-rich	4.00	Wepg	4.288	-2.346	-1.053	4.392
Hf 2-2	005.1-08.9	4.23	C-bin.	O(H)3 + ?	18.60	CK71	4.162	0.374	-0.654	3.856
Hu 1-1	119.6-06.7	7.55	Bin.	A? + ?	5.00	Wes05	-3.71	6.515	-0.887	13.401
Hu 1-2	086.5-08.8	4.33	Non-bin.	—	8.30	Liu04A	0.258	4.271	-0.665	8.842
Hu 2-1	051.4+09.6	5.06	Bin.	WNb + ?	2.60	RP22; Wes05	3.106	3.903	0.851	6.259
IC 351	159.0-15.1	4.86	Non-bin.	O(H)f	7.00	Wes05	-4.38	1.676	-1.273	12.493
IC 418	215.2-24.2	1.40	Non-bin.	O(H)f	12.00	CK71	-1.043	-0.736	-0.576	9.073
IC 1747	130.2+01.3	2.58	Non-bin.	[WO 4]	13.00	Wes05	-1.667	1.968	0.063	9.865
IC 2003	161.2-14.8	4.31	Non-bin.	[WC 3]?	8.60	Wes05	-3.945	1.338	-1.108	12.019
IC 3568	123.6+34.5	2.41	Non-bin.	O(H)3	10.00	Liu04A	-1.099	1.654	1.365	9.248
IC 4191	304.5-04.8	2.82	Non-bin.	—	5.00	PK67	1.595	-2.313	-0.237	6.810
IC 4406	319.6+15.7	1.15	Non-bin.	[WR]	35.00	PK67	0.844	-0.716	0.312	7.192
IC 4593	025.3+40.8	3.15	Non-bin.	O(H)5f	13.00	CK71	2.154	1.020	2.060	5.934
IC 4663	346.2-08.2	2.70	Non-bin.	[WN 3]	15.67	Boj21	-0.748	-1.953	-2.505	8.964
IC 4699	348.0-13.8	5.59	Non-bin.	O(H)3 V((f))	5.00	CK71	5.309	-1.127	-1.338	2.917
IC 4776	002.1-13.4	4.72	Bin.	O + ?	7.50	CK71	4.588	0.168	-1.097	3.416
IC 4846	027.64-9.6	6.10	Non-bin.	O(H)3-4 f	2.00	CK71	5.328	2.790	-1.021	3.863
IC 4997	058.3-10.9	5.15	Non-bin.	wels	2.50	Wepg	2.654	4.303	-0.981	6.862
IC 5217	100.6-05.4	4.68	Non-bin.	[WC]?	6.60	Wes05	-0.859	4.579	-0.44	9.972
K 648	065.0-27.3	10.12	Non-bin.	sdO	1.00	PK67	3.801	8.150	-4.642	9.169
M 1-20	006.1+08.3	7.07	Non-bin.	wels	2.50	Wepg	6.954	0.753	1.028	1.289
M 1-25	004.9+04.9	5.60	Non-bin.	[WC 5-6]	4.60	CK71	5.559	0.480	0.482	2.488
M 1-29	359.1-01.7	3.32	Non-bin.	—	7.60	WL07	3.318	-0.052	-0.099	4.682
M 1-30	355.9-04.2	5.80	Non-bin.	wels	5.00	PK67	5.769	-0.414	-0.431	2.269
M 1-31	006.4+02.0	5.16	Non-bin.	wels	—	—	5.124	0.579	0.181	2.934
M 1-32	011.9+04.2	3.56	Non-bin.	[WO 4]pec	7.60	CK71	3.473	0.736	0.263	4.586
M 1-33	013.1+04.1	5.88	Non-bin.	—	4.80	CK71	5.712	1.330	0.426	2.647
M 1-42	002.7-04.8	4.37	Non-bin.	cont.	9.00	Liu04B	4.349	0.207	-0.369	3.656
M 1-60	019.7-04.5	6.77	Non-bin.	[WC 4]	10.00	KO90	6.350	2.285	-0.534	2.818
M 1-61	019.4-05.3	5.40	Non-bin.	wels	1.80	WL07	5.071	1.786	-0.503	3.430
M 1-73	051.9-03.8	5.32	Non-bin.	O(H)3.5 If	5.00	Wes05	3.275	4.177	-0.358	6.306
M 1-74	052.2-04.0	9.43	Non-bin.	WN b?	5.00	Wes05	5.763	7.435	-0.659	7.764
M 2-4	349.8+04.4	7.11	Non-bin.	—	5.00	WL07	6.976	-1.255	0.553	1.620
M 2-6	353.3+06.3	6.68	Non-bin.	—	8.00	WL07	6.595	-0.769	0.734	1.602
M 2-23	002.2-02.7	5.05	Non-bin.	Of	8.50	WL07	5.040	0.195	-0.245	2.966
M 2-24	356.9-05.8	9.46	Non-bin.	—	6.80	CK71	9.399	-0.496	-0.956	1.484

Continue

Table A1 – Continued

Name	PN G	Distance (kpc)	Binarity	CSPN	Diameter (arcsec)	Diam. ref.	X _G (kpc)	Y _G (kpc)	Z _G (kpc)	R _G (kpc)
M 2-27	359.9–04.5	6.26	Non-bin.	[WC 4]:	4.80	WL07	6.240	-0.005	-0.501	1.760
M 2-31	006.0–03.6	5.94	Non-bin.	[WC 4]	5.10	Mor88	5.895	0.624	-0.375	2.195
M 2-33	002.0–06.2	8.19	Non-bin.	O(H)5f	5.80	WL07	8.137	0.287	-0.887	0.318
M 2-36	003.2–06.1	6.17	Non-bin.	—	8.00	Liu01	6.124	0.351	-0.665	1.909
M 2-39	008.1–04.7	8.61	Non-bin.	wels	3.20	WL07	8.494	1.215	-0.713	1.312
M 2-42	008.2–04.8	7.34	Non-bin.	wels:	3.80	WL07	7.239	1.046	-0.619	1.293
M 3-7	357.1+03.6	5.40	Non-bin.	wels	5.80	WL07	5.382	-0.271	0.340	2.631
M 3-15	006.8+04.1	5.34	Non-bin.	[WC 4]	4.20	CK71	5.288	0.631	0.387	2.784
M 3-21	355.1–06.9	6.41	Non-bin.	—	5.00	WL07	6.340	-0.543	-0.776	1.747
M 3-27	043.3+11.6	6.53	Non-bin.	EL	1.00	Wes05	4.650	4.390	1.323	5.522
M 3-29	004.0–11.1	5.73	Non-bin.	—	8.20	WL07	5.609	0.392	-1.103	2.423
M 3-32	009.4–09.8	6.70	Non-bin.	—	6.00	WL07	6.512	1.078	-1.15	1.837
M 3-33	009.6–10.6	6.94	Non-bin.	wels	5.00	WL07	6.724	1.141	-1.283	1.711
M 3-34	031.0–10.8	4.73	Non-bin.	—	5.60	Wes05	3.979	2.396	-0.894	4.681
Me 2-2	100.0–08.7	8.75	Non-bin.	Of	5.00	Wes05	-1.506	8.516	-1.333	12.763
MPA J1759-3007	000.5–03.1	7.62	C-bin.	—	25.00	Wegp	7.608	0.066	-0.423	0.398
MyCn 18	307.5–04.9	3.33	Bin.	O(H)f + ?	4.00	Boj21	2.021	-2.631	-0.287	6.532
NGC 40	120.0+09.8	1.98	Non-bin.	[WC 8]	48.00	Liu04A	-0.976	1.689	0.339	9.133
NGC 1501	144.5+06.5	1.18	Non-bin.	[WO 4]	52.00	CKS92	-0.955	0.680	0.135	8.981
NGC 2022	196.6–10.9	2.50	Non-bin.	O(H)	19.00	CK71	-2.351	-0.705	-0.474	10.375
NGC 2392	197.8+17.4	1.93	Bin.	O(H)6f + ?	46.00	CKS92	-1.753	-0.565	0.577	9.769
NGC 2440	234.8+02.4	1.48	Non-bin.	cont.	16.00	PK67	-0.852	-1.209	0.062	8.934
NGC 2867	278.1–05.9	2.24	Bin.	[WO 2] + ?	14.00	CK71	0.316	-2.206	-0.231	7.994
NGC 3132	272.1+12.3	1.25	Bin.	A2 V + ?	30.00	CJA87	0.045	-1.22	0.268	8.048
NGC 3242	261.0+32.0	1.41	Bin.	O(H) + ?	25.00	CJA87	-0.186	-1.181	0.748	8.271
NGC 3918	294.6+04.7	1.55	Non-bin.	O(H)?	19.00	CK71; Gar15		0.645	-1.404	0.127
NGC 5189	307.2–03.4	0.68	Bin.	[WO 1] + ?	140.00	CK71	0.410	-0.541	-0.041	7.609
NGC 5307	312.3+10.5	2.88	Non-bin.	O(H)3.5 V	12.50	CK71	1.908	-2.092	0.528	6.442
NGC 5315	309.1–04.3	2.09	Non-bin.	[WO 4]	6.00	CK71	1.315	-1.617	-0.16	6.878
NGC 5882	327.8+10.0	2.39	Non-bin.	O(H) f	14.00	CK71	1.991	-1.254	0.418	6.138
NGC 6153	341.8+05.4	1.48	Non-bin.	wels	24.00	CK71	1.400	-0.459	0.140	6.616
NGC 6210	043.1+37.7	2.20	Non-bin.	O(H)3	16.20	Liu04A	1.270	1.189	1.347	6.834
NGC 6302	349.5+01.0	0.65	Bin.	G V + ?	44.50	CK71	0.639	-0.118	0.012	7.362
NGC 6326	338.1–08.3	3.34	C-bin.	O(H)5-8 ((fc)) + ?	12.50	CK71	3.068	-1.228	-0.487	5.083
NGC 6337	349.3–01.1	1.82	C-bin.	wels + ?	51.00	CJA87	1.788	-0.336	-0.035	6.221
NGC 6369	002.4+05.8	1.14	Non-bin.	[WO 3]	38.00	CJA87	1.133	0.048	0.116	6.867
NGC 6439	011.0+05.8	6.31	Non-bin.	—	5.00	WL07	6.161	1.199	0.648	2.195
NGC 6543	096.4+29.9	1.37	Non-bin.	Of-WR(H)	19.50	Ack91	-0.134	1.180	0.684	8.219
NGC 6565	003.5–04.6	3.92	Non-bin.	—	13.60	WL07	3.900	0.241	-0.316	4.107
NGC 6567	011.7–00.6	2.86	Non-bin.	wels	7.60	WL07	2.800	0.582	-0.032	5.232
NGC 6572	034.6+11.8	1.86	Non-bin.	Of-WR(H)	10.80	Liu04A	1.498	1.034	0.382	6.584
NGC 6620	005.8–06.1	6.31	Non-bin.	cont.	8.00	WL07	6.241	0.643	-0.675	1.873
NGC 6644	008.3–07.3	4.95	Non-bin.	wels	2.60	CKS92	4.857	0.716	-0.63	3.223
NGC 6720	063.1+13.9	0.80	Non-bin.	hgO(H)	76.00	Liu04A	0.350	0.693	0.193	7.681
NGC 6741	033.8–02.6	3.29	Non-bin.	—	8.00	Liu04A	2.731	1.828	-0.154	5.577
NGC 6778	034.5–06.7	2.88	C-bin.	O(H)3-4 + ?	15.80	CK71	2.355	1.624	-0.337	5.874
NGC 6790	037.8–06.3	3.71	Non-bin.	WN?	7.00	Liu04A	2.910	2.265	-0.407	5.571
NGC 6803	046.4–04.1	4.95	Non-bin.	wels	5.50	Wes05	3.402	3.578	-0.356	5.826
NGC 6807	042.9–06.9	10.38	Non-bin.	Of	2.00	Wes05	7.541	7.022	-1.251	7.037
NGC 6818	025.8–17.9	1.88	Bin.	wels + ?	20.00	CK71	1.610	0.780	-0.578	6.438
NGC 6826	083.5+12.7	1.31	Non-bin.	O(H)3f + ?	25.00	Liu04A	0.143	1.269	0.290	7.959
NGC 6833	082.5+11.3	11.34	Non-bin.	Of	2.00	Wes05	1.445	11.024	2.230	12.826
NGC 6879	057.2–08.9	6.12	Non-bin.	O(He)3 f	5.00	Wes05	3.273	5.083	-0.948	6.941
NGC 6884	082.1+07.0	3.22	Non-bin.	WN b?	6.00	Liu04A	0.438	3.165	0.397	8.198
NGC 6891	054.1–12.1	2.83	Non-bin.	O(H)3 Ib(f*)	15.00	Wes05	1.619	2.244	-0.594	6.764
NGC 7009	037.7–34.5	1.30	Non-bin.	O(H)	28.00	CKS92	0.846	0.656	-0.738	7.184
NGC 7026	089.0+00.3	3.46	Non-bin.	[WO 3]	20.00	Wes05	0.060	3.459	0.022	8.661
NGC 7027	084.9–03.4	0.78	Non-bin.	cont.	14.00	Ack91	0.069	0.775	-0.047	7.969
NGC 7662	106.5–17.6	1.87	Non-bin.	O(H)	17.00	Liu04A	-0.508	1.709	-0.565	8.678
Ou 5	086.9–03.4	5.29	C-bin.	K + ?	48.00	Cor15	0.285	5.273	-0.321	9.345
PB 8	292.4+04.1	5.25	Non-bin.	[WN/C]	5.00	CKS92	1.999	-4.84	0.381	7.710
PC 14	336.2–06.9	5.02	Non-bin.	[WO 4]	7.00	CK71	4.562	-2.004	-0.611	3.980
Pe 1-1	285.4+01.5	5.39	Non-bin.	[WC 5]	3.00	CK71	1.435	-5.193	0.141	8.371

Continue

Table A1 – Continued

Name	PN G	Distance (kpc)	Binarity	CSPN	Diameter (arcsec)	Diam. ref.	X _G (kpc)	Y _G (kpc)	Z _G (kpc)	R _G (kpc)
Pe 1-9	005.0+03.0	4.63	C-bin.	O(H) + ?	12.40	CK71	4.606	0.405	0.247	3.419
Sp 3	342.5–14.3	2.09	Bin.	O3 + ?	36.00	PK67	1.932	-0.609	-0.517	6.099
Sp 4-1	068.7+14.8	21.51	Non-bin.	O?	—	—	7.527	19.386	5.495	19.392
Vy 1-2	053.3+24.0	8.81	Bin.	[WR]/wels + ?	4.60	RP22; Wes05	4.802	6.455	3.590	7.203
Vy 2-1	007.0–06.8	6.69	Non-bin.	wels	7.00	WL07	6.592	0.814	-0.796	1.626
Vy 2-2	045.4–02.7	4.39	Non-bin.	B[e]	3.10	RP22	3.074	3.127	-0.207	5.835
Wray 16-423	006.8–19.8	17.34	Non-bin.	—	2.60	Ots15B	16.192	1.951	-5.891	8.421

Distances from Hernández-Juárez et al. (2024).

CSPN classifications from Weidmann et al. (2020).

References: Ack91: Acker et al. (1991), Boj21: Bojičić et al. (2021), CK71: Cahn & Kaler (1971), CJA87: Chu et al. (1987), CPT87: Clegg et al. (1987), Cor15: Corradi et al. (2015), Gar15: García-Rojas et al. (2015), KO90: Kapusta & Olive (1990), KM81 Kohoutek & Martin (1981), Liu01: Liu et al. (2001), Liu04A: Liu et al. (2004a), Liu04B: Liu et al. (2004b), Mor88: Moreno et al. (1988), Ots10: Otsuka et al. (2010), Ots15B: Otsuka (2015), PK67: Perek & Kohoutek (1967), RP22: Ruiz-Escobedo & Peña (2022), WL07: Wang & Liu (2007), Wes05: Wesson et al. (2005), Wes08: Wesson et al. (2008), Wepg: Wesson (2024).

Table A2: Line ratios from the literature and calculated electron densities from [S II] and [Cl III] lines with PyNEB. A $T_e = 10^4$ K was assumed for all calculations.

Name	[S II] 6731/6716	[Cl III] 5537/5517	Reference	n_e ([S II]) (cm $^{-3}$)	n_e ([Cl III]) (cm $^{-3}$)
Abell 46	0.90	—	Cor15	313	—
Abell 58	1.40	—	Wes08	1628	—
Abell 63	1.08	—	Cor15	666	—
BoBn 1	1.51	—	Ots10	2140	—
Cn 1-5 (a)	1.72	1.18	WL07	3611	3200
Cn 1-5 (b)*	1.76	1.22	Gar12	4020	3504
Cn 2-1	1.72	1.18	WL07	3611	3200
DdDm 1 (a)*	1.69	0.40	Ots09	3344	—
DdDm 1 (b)	2.71	—	Wes05	—	—
Fg 1	0.89	—	Wes18	297	—
H 1-35	2.17	3.14	WL07	20378	35502
H 1-40	1.99	1.35	Gar18	8257	4530
H 1-41	1.23	0.89	WL07	1048	1192
H 1-42	1.85	1.45	WL07	5185	5381
H 1-50 (a)*	1.92	1.97	Gar18	6455	10780
H 1-50 (b)	1.85	1.79	WL07	5185	8693
H 1-54	2.00	2.16	WL07	8575	13259
H 4-1	1.14	1.00	Ots13	806	1913
Hb 4	1.90	1.51	Gar12	6058	5914
Hen 2-118	1.94	1.97	WL07	6909	10780
Hen 2-155	1.22	—	Jon15	1018	—
Hen 2-158	1.62	1.47	Gar18	2806	5550
Hen 2-161	1.27	—	Jon15	1168	—
Hen 2-283	1.71	—	Wes18	3525	—
Hen 2-436	2.25	2.81	Ots11	45827	25560
Hen 2-73	1.93	1.94	Gar18	6683	10412
Hen 2-86	2.13	2.46	Gar12	15798	18072
Hen 2-96	2.04	2.56	Gar18	10087	19981
Hen 3-1357 (a)	2.06	2.05	Ots17	11044	11785
Hen 3-1357 (b)	1.93	—	Pen22	6683	—
Hen 3-1357 (c)*	1.92	2.20	Pen22	6455	13853
Hf 2-2 (b)*	0.92	0.97	McN16	347	1716
Hu 1-1	1.25	0.66	Wes05	1107	—
Hu 1-2	1.67	1.27	Liu04A	3167	3889
Hu 2-1 (a)*	2.31	2.08	RP22	—	12184
Hu 2-1 (b)	2.35	—	Wes05	—	—
IC 351	1.75	—	Wes05	3912	—
IC 418	2.12	1.96	Sha04	14917	10651
IC 1747	1.71	—	Wes05	3525	—
IC 2003	1.70	0.93	Wes05	3431	1450
IC 3568	1.29	—	Liu04A	1232	—
IC 4191 (a)*	1.99	2.10	Tsa03	8257	12444
IC 4191 (b)	1.08	1.92	Tsa03	666	10156
IC 4406	1.13	1.22	Tsa03	781	3504
IC 4593	1.23	0.82	Rob05	1048	752
IC 4663	1.52	0.65	Moh23	2182	—
IC 4699	1.52	0.65	WL07	2182	—
IC 4776	2.07	2.49	Sow17	11556	18626
IC 4846 (a)*	1.83	1.36	WL07	4907	4620
IC 4846 (b)	2.07	—	Wes05	11556	—
IC 4997	2.17	—	—	20378	—
IC 5217	0.49	—	Wes05	—	—
K 648	1.53	1.33	Ots15A	2242	4362
M 1-20	1.93	1.80	WL07	6683	8798
M 1-25	1.99	0.06	Gar12	8257	—
M 1-29	1.59	1.35	WL07	2600	4530
M 1-30	1.90	1.63	Gar12	6058	7046
M 1-31	1.80	2.42	Gar18	4496	17350
M 1-32	2.08	2.06	Gar12	12110	11911
M 1-33	1.79	1.55	Gar18	4375	6273
M 1-42 (a)*	1.21	0.95	Liu01	990	1584
M 1-42 (b)	1.24	0.94	McN16	1077	1515

Continue

Table A2 – Continued

Name	[S II] 6731/6716	[Cl III] 5537/5517	Reference	n_e ([S II]) (cm $^{-3}$)	n_e ([Cl III]) (cm $^{-3}$)
M 1-60	1.91	2.05	Gar18	6244	11785
M 1-61 (a)*	2.17	2.36	Gar12	20378	16332
M 1-61 (b)	2.08	2.45	WL07	12110	17909
M 1-73	1.80	—	Wes05	4496	—
M 1-74	2.09	—	Wes05	12729	—
M 2-4	1.82	1.60	WL07	4761	6744
M 2-6	1.86	0.85	WL07	5345	939
M 2-23	2.05	2.05	WL07	10539	11785
M 2-24	1.32	—	Zha03	1333	—
M 2-27	1.87	2.13	WL07	5517	12865
M 2-31	1.81	1.75	Gar18	4620	8257
M 2-33	1.33	0.55	WL07	1367	—
M 2-36 (a)	1.66	1.41	Liu01	3096	5027
M 2-36 (b)*	1.61	1.34	Esp21	2737	4448
M 2-39	1.72	0.93	WL07	3611	1450
M 2-42	1.58	1.15	WL07	2538	2972
M 3-7	1.77	1.11	WL07	4119	2688
M 3-15	1.88	1.72	Gar12	5720	7951
M 3-21	1.98	1.96	WL07	7963	10651
M 3-27 (b)*	1.27	—	RPB24	1168	—
M 3-29	1.08	0.58	WL07	666	—
M 3-32	1.50	0.84	WL07	2089	877
M 3-33	1.15	0.94	WL07	831	1515
Me 2-2	1.10	—	Wes05	710	—
MPA J1759-3007	1.10	—	Wes18	710	—
MyCn 18	1.76	1.91	Tsa03	4020	10034
NGC 40	1.37	0.84	Liu04A	1512	877
NGC 1501	1.10	0.95	Erc04	710	1584
NGC 2022	1.12	0.96	Tsa03	757	1650
NGC 2392 (a)	1.56	0.94	Zha12	2415	1515
NGC 2392 (b)*	1.08	0.87	Zha12	666	1067
NGC 2440	1.94	—	Tsa03	6909	—
NGC 2867 (a)*	1.63	1.23	Gar09	2870	3573
NGC 2867 (b)	1.49	1.24	Gar09	2033	3650
NGC 3132	0.98	0.82	Tsa03	458	752
NGC 3242	1.41	0.91	Tsa03	1670	1319
NGC 3918 (a)	1.74	1.43	Tsa03	3813	5197
NGC 3918 (b)*	1.82	1.49	Gar15	4761	5720
NGC 5189	1.21	0.88	Gar12	990	1129
NGC 5307	1.78	0.94	Rui03	4245	1515
NGC 5315 (a)*	2.01	2.90	Ma17	8865	27900
NGC 5315 (b)	1.89	2.70	Tsa03	5860	22926
NGC 5882	1.72	1.21	Tsa03	3611	3420
NGC 6153 (a)*	1.66	1.27	Liu00	3096	3889
NGC 6153 (b)	1.68	0.44	McN16	3264	—
NGC 6210 (b)	1.66	1.17	Liu04A	3096	3124
NGC 6302	1.96	2.54	Tsa03	7440	19593
NGC 6326	1.12	—	Wes18	757	—
NGC 6337	0.91	—	Wes18	330	—
NGC 6369	1.67	1.21	Gar12	3167	3420
NGC 6439	1.74	1.40	WL07	3813	4945
NGC 6543S	1.85	1.40	Wes04	5185	4945
NGC 6565	1.34	0.95	WL07	1401	1584
NGC 6567	1.83	2.17	WL07	4907	13441
NGC 6572	2.11	1.25	Liu04A	14042	3733
NGC 6620	1.49	1.12	WL07	2033	2754
NGC 6720	0.96	0.78	Liu04A	420	509
NGC 6741	1.74	1.37	Liu04A	3813	4697
NGC 6778	1.06	—	Jon16	621	—
NGC 6790	2.19	2.46	Liu04A	24280	18072
NGC 6803	1.88	1.81	Wes05	5720	8905
NGC 6807	2.03	—	Wes05	9669	—
NGC 6818	1.33	1.05	Tsa03	1367	2263
NGC 6826	1.37	0.91	Liu04A	1512	1319

Continue

Table A2 – Continued

Name	[S II] 6731/6716	[Cl III] 5537/5517	Reference	n_e ([S II]) (cm $^{-3}$)	n_e ([Cl III]) (cm $^{-3}$)
NGC 6884	1.88	1.42	Liu04A	5720	5127
NGC 7009	1.66	1.20	Fan11	3096	3344
NGC 7026	2.33	1.82	Wes05	—	9014
NGC 7027	2.25	3.42	Zha05	45827	47879
NGC 7662	1.50	1.00	Liu04A	2089	1913
Ou 5	0.80	—	Cor15	154	—
PB 8	1.51	1.00	Gar09	2140	1913
PC 14	1.66	1.16	Gar12	3096	3045
Pe 1-1	2.11	2.75	Gar12	14042	24098
Pe 1-9	0.96	—	Wes18	420	—
Sp 3	1.10	0.88	Mis19	710	1129
Vy 1-2 (a)*	1.88	1.97	RP22	5720	10780
Vy 1-2 (b)	1.22	—	Wes05	1018	—
Vy 2-1	1.61	1.43	WL07	2737	5197
Vy 2-2 (a)*	1.95	3.83	RP22	7121	79237
Vy 2-2 (b)	3.02	—	Wes05	—	—
Wray 16-423	1.67	1.48	Ots15B	3167	5643

* Adopted values for ionized mass calculations.

References: Cor15: Corradi et al. (2015), Erc04: Ercolano et al. (2004), Esp21: Espíritu & Peimbert (2021), Fan11: Fang & Liu (2011), Gar09: García-Rojas et al. (2009), Gar12: García-Rojas et al. (2012), Gar15: García-Rojas et al. (2015), Gar18: García-Rojas et al. (2018), Jon15: Jones et al. (2015), Jon16: Jones et al. (2016), Liu00: Liu et al. (2000), Liu04A: Liu et al. (2004a), Liu06: Liu et al. (2006), Ma17: Madonna et al. (2017), McN16: McNabb et al. (2016), Mis19: Miszalski et al. (2019), Moh23: Mohery et al. (2023), Ots09: Otsuka et al. (2009), Ots10: Otsuka et al. (2010), Ots11: Otsuka et al. (2011), Ots13: Otsuka & Tajitsu (2013), Ots15A: Otsuka et al. (2015), Ots15B: Otsuka (2015), Ots17: Otsuka et al. (2017), Pen22: Peña et al. (2022), Rob05: Robertson-Tessi & Garnett (2005), Rui03: Ruiz et al. (2003), RP22: Ruiz-Escobedo & Peña (2022), RPB24: Ruiz-Escobedo et al. (2024), Sha04: Sharpee et al. (2004), Sim22: Simpson et al. (2022), Sow17: Sowicka et al. (2017), Tsa03: Tsamis et al. (2003), WL07: Wang & Liu (2007), Wes03: Wesson et al. (2003), Wes04: Wesson & Liu (2004), Wes05: Wesson et al. (2005), Wes18: Wesson et al. (2018), Zha05: Zhang et al. (2005), Zha12: Zhang et al. (2012).

Table A3: $c(H\beta)$, sizes of employed slits for $H\beta$ Flux, total fluxes and $L(H\beta)$

Name	$c(H\beta)$	Ref. $c(H\beta)$	Slit size (arcsec)	$F(H\beta)$ Slit ($\text{erg cm}^{-2} \text{s}^{-1}$)	Ref. $F(H\beta)$ Slit	$L(H\beta)$ Slit (L_\odot)	$F(H\beta)$ Global ($\text{erg cm}^{-2} \text{s}^{-1}$)	Ref. $F(H\beta)$ Global	$L(H\beta)$ Global (L_\odot)
Abell 30 (J1)*	1.02	Wes03	0.82	1.24E-16	Wes03	2.20E-4	6.46E-13	Kal83b	1.15
Abell 30 (J3)	0.64	Wes03	0.82	1.49E-16	Wes03	1.10E-4	6.46E-13	Kal83b	0.48
Abell 30 (J4)	1.26	Sim22	0.82	1.37E-16	Sim22	4.22E-4	6.46E-13	Kal83b	1.99
Abell 46	0.22	Cor15	1.00	3.53E-14	Cor15	0.01	1.41E-12	Kal83b	0.43
Abell 58	1.04	Wes08	1.00	3.80E-17	Wes08	4.02E-4	—	—	—
Abell 63	0.55	Cor15	1.00	1.80E-14	Cor15	0.02	1.58E-13	Ack91	0.15
BoBn 1	0.09	Ots10	1.20	2.95E-13	Ots10	4.33	2.00E-13	Ack91	2.93
Cn 1-5 (a)	0.49	WL07	2.00	3.98E-12	WL07	7.65	6.17E-12	Ack91	11.86
Cn 1-5 (b)*	0.56	Gar12	1.00	9.72E-13	Gar12	2.20	6.17E-12	Ack91	13.94
Cn 2-1	1.07	WL07	2.00	2.34E-12	WL07	36.81	2.34E-12	Web83	36.81
DdDm 1 (a)*	0.06	Hen08	0.60	1.86E-12	Ots09	19.30	2.69E-12	Ack91	27.91
DdDm 1 (b)	0.14	Wes05	1.00	2.69E-12	Wes05	33.56	2.69E-12	Ack91	33.56
Fg 1	0.52	Wes18	—	—	—	—	8.71E-12	Per71	6.43
H 1-35	1.51	WL07	2.00	3.16E-12	WL07	100.80	3.55E-12	Ack91	113.24
H 1-40	2.41	Gar18	1.30	1.41E-13	Gar18	68.53	2.57E-13	Ack91	124.91
H 1-41	0.65	WL07	2.00	1.26E-12	WL07	4.86	2.00E-12	Ack91	7.71
H 1-42	0.87	WL07	2.00	2.09E-12	WL07	12.29	2.00E-12	Ack91	11.76
H 1-50 (a)*	0.88	Gar18	1.30	1.79E-12	Gar18	36.05	2.09E-12	Ack91	42.09
H 1-50 (b)	0.68	WL07	2.00	1.99E-12	WL07	25.29	2.09E-12	Ack91	26.56
H 1-54	1.54	WL07	2.00	1.35E-12	WL07	100.47	1.32E-12	Web83	98.24
H 4-1	0.10	Ots13	0.60	3.86E-13	Ots13	4.41	5.37E-13	Ack91	6.14
Hb 4	1.81	Gar12	1.00	1.34E-13	Gar12	3.80	1.12E-12	Sha89	31.74
Hen 2-73	1.39	Gar18	1.30	9.11E-13	Gar09	26.30	1.12E-12	Ack91	32.34
Hen 2-86	2.10	Gar12	1.00	2.96E-13	Gar12	23.80	3.16E-14	Ack91	2.54
Hen 2-96	2.01	Gar18	1.00	3.35E-13	Gar18	28.16	4.27E-13	Ack91	35.89
Hen 2-118	0.17	WL07	2.00	2.14E-12	WL07	16.03	2.00E-12	Sha89	14.98
Hen 2-155	0.74	Jon15	—	—	—	—	2.57E-12	Sha89	3.83
Hen 2-158	0.56	Gar18	1.30	1.01E-12	Gar18	27.91	7.59E-13	Web69	20.98
Hen 2-161	1.21	Jon15	—	—	—	—	7.94E-13	Web69	8.37
Hen 2-283	1.48	Wes18	—	—	—	—	1.82E-13	Ack91	12.97
Hen 2-436	0.23	Ots11	—	—	—	—	6.76E-13	Web83	27.53
Hen 3-1357 (a)	0.16	Ots17	2.00	9.84E-12	Ots17	10.64	—	—	—
Hen 3-1357 (b)	0.15	Pen22	2.00	9.84E-12	Ots17	10.40	—	—	—
Hen 3-1357 (c)*	0.22	Pen22	2.00	9.84E-12	Ots17	12.21	—	—	—
Hf 2-2 (a)	0.47	Liu06	—	—	—	—	5.01E-13	Ack91	0.79
Hf 2-2 (b)*	0.47	Liu06	—	—	—	—	5.01E-13	Ack91	0.79
Hf 2-2 (c)	0.33	Wes18	—	—	—	—	5.01E-13	Ack91	0.57
Hu 1-1	0.55	Wes05	1.00	2.51E-12	Wes05	15.19	2.51E-12	Bar78	15.19
Hu 1-2	0.51	Liu04A	1.00	6.17E-12	Liu04A	11.20	6.17E-12	Kal76	11.20
Hu 2-1 (a)*	0.45	RP22	1.00	1.58E-11	Wes05	34.11	1.58E-11	KM81	34.11
Hu 2-1 (b)	0.78	Wes05	1.00	1.58E-11	Wes05	72.93	1.58E-11	KM81	72.93
IC 351	0.38	Wes05	1.00	3.80E-12	Wes05	6.44	3.80E-12	Bar78	6.44
IC 418	0.34	Sha04	—	—	—	—	2.63E-10	Sha89	33.74
IC 1747	1.00	Wes05	1.00	3.24E-12	Wes05	6.45	3.24E-12	ODE63	6.45
IC 2003	0.35	Wes05	1.00	6.46E-12	Wes05	8.04	6.46E-12	Bar78	8.04
IC 3568	0.26	Liu04A	1.00	1.51E-11	Liu04A	4.77	1.51E-11	Kal76	4.77
IC 4191 (a)*	0.70	Tsa03	2.00	1.02E-11	Tsa03	12.16	1.00E-11	Sha89	11.92
IC 4191 (b)	0.70	Tsa03	2.00	1.02E-11	Tsa03	12.16	1.00E-11	Sha89	11.92
IC 4406	0.27	Tsa03	2.00	1.78E-11	Tsa03	1.31	1.82E-11	Web83	1.34
IC 4593	0.17	Rob05	2.50	2.63E-11	Rob05	11.55	2.63E-11	Web83	11.55
IC 4663	0.54	Moh23	—	—	—	—	3.80E-12	Moh23	2.87
IC 4699	0.23	WL07	2.00	2.00E-12	WL07	3.18	2.04E-12	Sha89	3.24
IC 4776	0.22	Sow17	—	—	—	—	1.91E-11	Web83	21.13
IC 4846 (a)*	0.69	WL07	2.00	5.01E-12	WL07	27.32	4.57E-12	Sha89	24.92
IC 4846 (b)	0.70	Wes05	1.00	4.57E-12	Wes05	25.50	4.57E-12	Sha89	25.50
IC 4997	0.32	RP22	—	—	—	—	2.95E-11	Kal78	48.91
IC 5217	0.50	Wes05	1.00	6.76E-12	Wes05	14.01	6.76E-12	Bar78	14.01
K 648	0.12	Ots15A	1.20	7.83E-13	Ots15A	3.16	7.94E-13	Haw78	3.21
M 1-20	1.40	WL07	2.00	1.14E-12	WL07	42.82	1.17E-12	Sha89	43.95
M 1-25	1.41	Gar12	1.00	5.01E-13	Gar12	12.08	1.20E-12	Ack91	28.94
M 1-29	2.03	WL07	2.00	3.89E-13	WL07	13.75	6.31E-13	Ack91	22.30
M 1-30	1.00	Gar12	1.00	5.20E-13	Gar12	5.23	1.70E-12	Ack91	17.11
M 1-31	2.08	Gar18	1.30	3.84E-13	Gar18	36.78	1.26E-12	Ack91	120.67

Continue

Table A3 – Continued

Name	c(H β)	Ref. c(H β)	Slit size (arcsec)	F(H β) Slit (erg cm $^{-2}$ s $^{-1}$)	Ref. F(H β) Slit	L(H β) Slit (L $_{\odot}$)	F(H β) Global (erg cm $^{-2}$ s $^{-1}$)	Ref. F(H β) Global	L(H β) Global (L $_{\odot}$)
M 1-32	1.30	Gar12	1.00	2.01E-13	Gar12	1.52	6.31E-13	Ack91	4.77
M 1-33	1.56	Gar18	1.30	8.65E-13	Gar18	32.49	8.13E-13	Ack91	30.53
M 1-42 (a)*	0.70	Liu04B	1.00	2.34E-12	Liu04B	6.70	2.40E-12	Web83	6.87
M 1-42 (b)	0.70	Liu04B	1.00	2.34E-12	Liu04B	6.70	2.40E-12	Web83	6.87
M 1-60	1.68	Gar18	1.30	6.25E-13	Gar18	41.02	5.25E-13	Ack91	34.46
M 1-61 (a)*	1.24	Gar12	1.00	2.45E-12	Gar12	37.14	3.72E-12	Ack91	56.40
M 1-61 (b)	0.92	WL07	2.00	3.47E-12	WL07	25.18	3.72E-12	Ack91	26.99
M 1-73	1.14	Wes05	1.00	2.00E-12	Wes05	23.38	2.00E-12	Ack91	23.38
M 1-74	1.12	Wes05	1.00	1.78E-12	Wes05	62.43	1.78E-12	Bar78	62.43
M 2-4	1.33	WL07	2.00	1.15E-12	WL07	37.19	1.45E-12	Ack91	46.89
M 2-6	1.14	WL07	2.00	5.89E-13	WL07	10.85	1.26E-12	Ack91	23.22
M 2-23	1.20	WL07	2.00	2.63E-12	WL07	31.80	2.69E-12	Web83	32.53
M 2-24	0.80	Zha03	2.00	7.94E-13	Zha03	13.41	8.13E-13	Ack91	13.73
M 2-27	1.31	WL07	2.00	5.89E-13	WL07	14.10	6.31E-13	Ack91	15.10
M 2-31	1.43	Gar18	1.30	7.02E-13	Gar18	19.95	7.76E-13	Via85	22.05
M 2-33	0.55	WL07	2.00	1.41E-12	WL07	10.04	2.51E-12	Ack91	17.87
M 2-36 (a)	0.27	Liu04B	2.00	3.54E-12	Liu01	7.51	6.31E-12	Ack91	13.38
M 2-36 (b)*	0.33	Esp21	2.00	3.54E-12	Liu01	8.62	6.31E-12	Ack91	15.37
M 2-39	0.61	WL07	2.00	8.51E-13	WL07	7.69	7.41E-13	Ack91	6.70
M 2-42	1.06	WL07	2.00	7.94E-13	WL07	14.69	7.59E-13	Ack91	14.05
M 3-7	1.65	WL07	2.00	4.17E-13	WL07	16.25	5.13E-13	Web83	19.99
M 3-15	2.09	Gar12	1.00	9.01E-13	Gar12	94.57	3.55E-13	Ack91	37.26
M 3-21	0.50	WL07	2.00	4.07E-12	WL07	15.82	3.80E-12	Sha89	14.77
M 3-27 (a)	—	—	1.00	1.48E-12	Wes05	—	1.48E-12	Bar78	—
M 3-27 (b)*	0.63	RPB24	1.00	—	—	—	5.50E-12	KM81	29.93
M 3-29	0.24	WL07	2.00	1.66E-12	WL07	2.83	2.51E-12	Ack91	4.28
M 3-32	0.64	WL07	2.00	1.41E-12	WL07	8.27	1.26E-12	Ack91	7.39
M 3-33	0.50	WL07	2.00	1.17E-12	WL07	5.33	1.00E-12	Ack91	4.56
M 3-34	0.58	Wes05	1.00	1.58E-12	Wes05	4.02	1.58E-12	Ack91	4.02
Me 2-2	0.34	Wes05	1.00	6.92E-12	Wes05	34.68	6.92E-12	Bar78	34.68
MPA J1759-3007	1.46	Wes18	—	—	—	—	—	—	—
MyCn 18	0.74	Tsa03	2.00	6.17E-12	Tsa03	11.25	7.41E-12	Web69	13.51
NGC 40	0.70	Liu04A	1.00	4.27E-11	Liu04A	25.10	2.19E-11	Lil55	12.87
NGC 1501	1.00	Erc04	—	—	—	—	5.25E-12	Col61	2.19
NGC 2022	0.42	Tsa03	2.00	7.41E-12	Tsa03	3.64	7.41E-12	KM81	3.64
NGC 2392 (a)	0.27	Zha12	—	—	—	—	4.07E-11	Sha85	8.45
NGC 2392 (b)*	0.27	Zha12	—	—	—	—	4.07E-11	Sha85	8.45
NGC 2440	0.47	Tsa03	2.00	3.16E-11	Tsa03	6.11	3.16E-11	Sha89	6.11
NGC 2867 (a)*	0.39	Gar09	—	—	—	—	2.63E-11	Sha89	9.69
NGC 2867 (b)	0.43	Gar09	—	—	—	—	2.63E-11	Sha89	10.63
NGC 3132	0.30	Tsa03	2.00	3.55E-11	Tsa03	3.31	3.55E-11	Web69	3.31
NGC 3242	0.17	Tsa03	2.00	1.62E-10	Tsa03	14.25	1.62E-10	Sha89	14.25
NGC 3918 (a)	0.40	Tsa03	2.00	9.12E-11	Tsa03	16.47	9.12E-11	KM81	16.47
NGC 3918 (b)*	0.27	Gar15	1.00	5.54E-12	Gar15	0.74	9.12E-11	KM81	12.21
NGC 5189	0.47	Gar12	1.00	1.17E-13	Gar09	4.78E-3	3.02E-11	Via85	1.23
NGC 5307	0.59	Rui03	3.00	1.18E-12	Rui03	1.14	6.61E-12	Web83	6.38
NGC 5315 (a)*	0.63	Ma17	—	—	—	—	3.80E-11	KM81	21.18
NGC 5315 (b)	0.55	Tsa03	2.00	3.80E-11	Tsa03	17.62	3.80E-11	KM81	17.62
NGC 5882	0.42	Tsa03	2.00	4.17E-11	Tsa03	18.74	4.27E-11	KM81	19.19
NGC 6153 (a)*	1.30	Liu00	—	—	—	—	1.45E-11	Web83	18.96
NGC 6153 (b)	1.32	McN16	—	—	—	—	1.45E-11	Web83	19.85
NGC 6210 (a)	0.53	Rob05	2.50	8.13E-11	Rob05	18.05	8.13E-11	KM81	18.05
NGC 6210 (b)*	0.13	Liu04A	1.00	8.13E-11	Liu04A	15.88	8.13E-11	KM81	15.88
NGC 6302	1.39	Tsa03	2.00	2.82E-11	Tsa03	8.75	2.82E-11	Per71	8.75
NGC 6326	0.47	Wes18	—	—	—	—	8.32E-12	Sha89	8.20
NGC 6337	0.50	Wes18	—	—	—	—	4.47E-12	Per71	1.40
NGC 6369	1.93	Gar12	1.00	6.72E-14	Gar12	0.22	4.79E-12	Per71	15.85
NGC 6439	1.10	WL07	2.00	1.86E-12	WL07	27.89	2.09E-12	Ack91	31.34
NGC 6543 (a)	0.08	Rob05	2.50	2.45E-10	Rob05	16.54	2.69E-10	Wes04	18.16
NGC 6543 (b)	0.08	Rob05	2.50	2.45E-10	Rob05	16.54	2.69E-10	Wes04	18.16
NGC 6543S (c)*	0.10	Wes04	—	—	—	—	2.69E-10	Wes04	19.02
NGC 6565	0.32	WL07	2.00	5.62E-12	WL07	5.40	6.03E-12	Sha89	5.79
NGC 6567	0.90	WL07	2.00	1.15E-11	WL07	22.35	1.17E-11	Sha89	22.74
NGC 6572 (a)	1.22	Rob05	2.50	1.51E-10	Rob05	259.38	1.51E-10	Sha89	259.38

Continue

Table A3 – Continued

Name	c(H β)	Ref. c(H β)	Slit size (arcsec)	F(H β) Slit (erg cm $^{-2}$ s $^{-1}$)	Ref. F(H β) Slit	L(H β) Slit (L $_{\odot}$)	F(H β) Global (erg cm $^{-2}$ s $^{-1}$)	Ref. F(H β) Global	L(H β) Global (L $_{\odot}$)
NGC 6572 (b)	1.22	Rob05	2.50	1.51E–10	Rob05	259.38	1.51E–10	Sha89	259.38
NGC 6572 (c)	1.22	Rob05	2.50	1.51E–10	Rob05	259.38	1.51E–10	Sha89	259.38
NGC 6572 (d)*	0.48	Liu04A	1.00	1.51E–10	Liu04A	47.20	1.51E–10	Sha89	47.20
NGC 6620	0.52	WL07	2.00	1.86E–12	WL07	7.34	1.86E–12	Web83	7.34
NGC 6644	—	—	—	—	—	—	1.02E–11	Sha89	—
NGC 6720 (a)*	0.20	Liu04A	1.00	8.32E–11	Liu04A	2.52	8.32E–11	Col61	2.52
NGC 6720 (b)	—	—	—	—	—	—	8.32E–11	Col61	—
NGC 6741	1.15	Liu04A	1.00	4.57E–12	Liu04A	20.90	4.79E–12	Web83	21.91
NGC 6778	0.46	Jon16	0.70	6.17E–12	Jon16	4.42	6.92E–12	Kal83b	4.95
NGC 6790 (a)	0.45	Rob05	2.50	1.26E–11	Rob05	14.62	1.26E–11	Kal83b	14.62
NGC 6790 (b)*	1.10	Liu04A	1.00	1.26E–11	Liu04A	65.32	1.26E–11	Kal83b	65.32
NGC 6803	0.87	Wes05	1.00	6.61E–12	Wes05	35.92	6.61E–12	Col61	35.92
NGC 6807	0.64	Wes05	1.00	3.31E–12	Wes05	46.58	3.31E–12	Kal80	46.58
NGC 6818	0.37	Tsa03	2.00	3.31E–11	Tsa03	8.21	3.31E–11	Web83	8.21
NGC 6826	0.06	Liu04A	1.00	1.10E–10	Liu04A	6.48	1.05E–10	Kal78	6.19
NGC 6833	0.00	Wes05	1.00	5.62E–12	Wes05	21.62	5.62E–12	Ack91	21.62
NGC 6879	0.40	Wes05	1.00	2.63E–12	Wes05	7.40	2.63E–12	Web83	7.40
NGC 6884	1.00	Liu04A	1.00	7.76E–12	Liu04A	24.07	7.76E–12	Col61	24.07
NGC 6891	0.29	Wes05	1.00	2.24E–11	Wes05	10.47	2.24E–11	Web83	10.47
NGC 7009 (a)	0.20	Liu95	—	—	—	—	1.66E–10	Web83	13.30
NGC 7009 (b)*	0.17	Fan11	—	—	—	—	1.66E–10	Web83	12.41
NGC 7026	1.12	Wes05	1.00	1.26E–11	Wes05	59.49	1.26E–11	Kal85	59.49
NGC 7027 (a)	0.92	Rob05	2.50	7.59E–11	Rob05	11.49	7.59E–11	Sha82	11.49
NGC 7027 (b)*	1.37	Zha05	—	—	—	—	7.59E–11	Sha82	32.39
NGC 7662	0.18	Liu04A	1.00	1.02E–10	Liu04A	16.15	1.02E–10	Kal78	16.15
Ou 5	0.94	Cor15	1.00	1.37E–14	Cor15	0.10	—	—	—
PB 8	0.36	Gar09	—	—	—	—	3.89E–12	Sha89	7.35
PC 14	0.63	Gar12	1.00	5.05E–13	Gar12	1.62	1.86E–12	Sha89	5.98
Pe 1-1	1.80	Gar12	1.00	2.57E–13	Gar12	14.09	5.50E–13	Ack91	30.16
Pe 1-9	1.35	Wes18	—	—	—	—	6.31E–14	Ack91	0.91
Sp 3	0.06	Mis19	—	—	—	—	7.94E–12	Ack91	1.19
Sp 4-1	0.00	Wes05	1.00	1.45E–12	Wes05	20.07	1.45E–12	Ack91	20.07
Vy 1-2 (a)*	0.31	RP22	1.00	2.95E–12	Wes05	13.99	2.95E–12	Kal80	13.99
Vy 1-2 (b)	0.14	Wes05	1.00	2.95E–12	Wes05	9.46	2.95E–12	Kal80	9.46
Vy 2-1	0.83	WL07	2.00	2.69E–12	WL07	24.35	3.16E–12	Ack91	28.61
Vy 2-2 (a)*	0.66	RP22	1.00	2.75E–12	Wes05	7.25	2.75E–12	Sha89	7.25
Vy 2-2 (b)	1.65	Wes05	1.00	2.75E–12	Wes05	70.83	2.75E–12	Sha89	70.83
Wray 16-423	0.13	Ots15B	1.20	1.53E–12	Ots15B	18.57	1.00E–12	Ack91	12.14

* Adopted values for ionized mass calculations.

References: Ack91: Acker et al. (1991), Bar78: Barker (1978), Col61: Collins et al. (1961), Cor15: Corradi et al. (2015), Erc04: Ercolano et al. (2004), Esp21: Espíritu & Peimbert (2021), Fan11: Fang & Liu (2011), Gar09: García-Rojas et al. (2009), Gar12: García-Rojas et al. (2012), Gar15: García-Rojas et al. (2015), Gar18: García-Rojas et al. (2018), Haw78: Hawley & Miller (1978), Hen08: Henry et al. (2008), Jon15: Jones et al. (2015), Jon16: Jones et al. (2016), Kal76: Kaler (1976), Kal78: Kaler (1978), Kal80: Kaler (1980), Kal83b: Kaler (1983), Kal85: Kaler & Lutz (1985), KM81: Kohoutek & Martin (1981), Lil55: Liller (1955), Liu95: Liu et al. (1995), Liu00: Liu et al. (2000), Liu04A: Liu et al. (2004a), Liu04B: Liu et al. (2004b), Liu06: Liu et al. (2006), Ma17: Madonna et al. (2017), Mis19: Miszalski et al. (2019), Moh23: Mohery et al. (2023), ODe63: O'Dell (1963), Ots10: Otsuka et al. (2010), Ots11: Otsuka et al. (2011), Ots15A: Otsuka et al. (2015), Ots15B: Otsuka (2015), Ots17: Otsuka et al. (2017), Pen22: Peña et al. (2022), Per71: Perek (1971), Rob05: Robertson-Tessi & Garnett (2005), Rui03: Ruiz et al. (2003), RP22: Ruiz-Escobedo & Peña (2022), RPB24: Ruiz-Escobedo et al. (2024), Sha04: Sharpee et al. (2004), Sha82: Shaw & Kaler (1982), Sha85: Shaw & Kaler (1985), Sha89: Shaw & Kaler (1989), Sim22: Simpson et al. (2022), Sow17: Sowicka et al. (2017), Tsa03: Tsamis et al. (2003), Via85: Viadana & de Freitas Pacheco (1985), WL07: Wang & Liu (2007), Web69: Webster (1969), Web83: Webster (1983), Wes03: Wesson et al. (2003), Wes04: Wesson & Liu (2004), Wes05: Wesson et al. (2005), Wes18: Wesson et al. (2018), Zha03: Zhang & Liu (2003), Zha05: Zhang et al. (2005), Zha12: Zhang et al. (2012).

Table A4: ADFs from the list by R. Wesson, ionized masses derived from the densities of [S II] and [Cl III] and the fluxes with slit or global, in solar units, are presented.

Name	ADF	Ref. ADF	$M_{ion}(\text{[S II]})$ Slit (M_\odot)	$M_{ion}(\text{[Cl III]})$ Slit (M_\odot)	$M_{ion}(\text{[S II]})$ Global (M_\odot)	$M_{ion}(\text{[Cl III]})$ Global (M_\odot)
Abell 30 (J1)*	770.00	Wes03	—	—	—	—
Abell 30 (J3)	600.00	Wes03	—	—	—	—
Abell 30 (J4)	22.00	Sim22	—	—	—	—
Abell 46	120.00	Cor15	1.29E-3	—	5.16E-2	—
Abell 58	90.00	Wes08	9.26E-6	—	—	—
Abell 63	8.00	Cor15	9.75E-4	—	8.56E-3	—
BoBn 1	3.05	Ots10	7.58E-2	—	5.14E-2	—
Cn 1-5 (a)	1.90	WL07	7.95E-2	8.97E-2	1.23E-1	1.39E-1
Cn 1-5 (b)*	1.60	Gar12	2.05E-2	2.35E-2	1.30E-1	1.49E-1
Cn 2-1	2.90	WL07	3.82E-1	4.31E-1	3.82E-1	4.31E-1
DdDm 1 (a)*	5.30	Ots09	2.16E-1	—	3.13E-1	—
DdDm 1 (b)	11.80	Wes05	—	—	—	—
Fg 1	46.00	Wes18	—	—	8.12E-1	—
H 1-35	2.10	WL07	1.85E-1	1.06E-1	2.08E-1	1.20E-1
H 1-40	2.88	Gar18	3.11E-1	5.67E-1	5.67E-1	1.03
H 1-41	5.10	WL07	1.74E-1	1.53E-1	2.76E-1	2.42E-1
H 1-42	2.30	WL07	8.89E-2	8.57E-2	8.51E-2	8.20E-2
H 1-50 (a)*	2.37	Gar18	2.09E-1	1.25E-1	2.45E-1	1.46E-1
H 1-50 (b)	2.90	WL07	1.83E-1	1.09E-1	1.92E-1	1.15E-1
H 1-54	2.60	WL07	4.39E-1	2.84E-1	4.30E-1	2.78E-1
H 4-1	1.75	Ots13	2.05E-1	8.65E-2	2.86E-1	1.20E-1
Hb 4	3.70	Gar12	2.35E-2	2.41E-2	1.96E-1	2.01E-1
Hen 2-118	1.70	WL07	8.70E-2	5.58E-2	8.13E-2	5.21E-2
Hen 2-155	6.30	Jon15	—	—	1.41E-1	—
Hen 2-158	1.61	Gar18	3.73E-1	1.89E-1	2.80E-1	1.42E-1
Hen 2-161	11.00	Jon15	—	—	2.69E-1	—
Hen 2-283	6.00	Wes18	—	—	1.38E-1	—
Hen 2-436	16.30	Ots11	—	—	2.25E-2	4.04E-2
Hen 2-73	2.29	Gar18	1.48E-1	9.47E-2	1.81E-1	1.16E-1
Hen 2-86	1.90	Gar12	5.65E-2	4.94E-2	6.03E-3	5.27E-3
Hen 2-96	1.41	Gar18	1.05E-1	5.29E-2	1.33E-1	6.74E-2
Hen 3-1357 (a)	1.51	Ots17	3.61E-2	3.39E-2	—	—
Hen 3-1357 (b)	2.52	Pen22	5.83E-2	—	—	—
Hen 3-1357 (c)*	3.47	Pen22	7.10E-2	3.31E-2	—	—
Hf 2-2 (a)	70.00	Liu06	—	—	—	—
Hf 2-2 (b)*	80.00	McN16	—	—	8.55E-2	1.73E-2
Hf 2-2 (c)	83.00	Wes18	—	—	—	—
Hu 1-1	2.97	Wes05	5.15E-1	—	5.15E-1	—
Hu 1-2	1.60	Liu04A	1.33E-1	1.08E-1	1.33E-1	1.08E-1
Hu 2-1 (a)*	1.85	RP22	—	1.05E-1	—	1.05E-1
Hu 2-1 (b)	4.00	Wes05	—	—	—	—
IC 351	3.14	Wes05	6.17E-2	—	6.17E-2	—
IC 418	2.00	Sha04	—	—	8.48E-2	1.19E-1
IC 1747	3.20	Wes05	6.86E-2	—	6.86E-2	—
IC 2003	7.31	Wes05	8.78E-2	2.08E-1	8.78E-2	2.08E-1
IC 3568	2.20	Liu04A	1.45E-1	—	1.45E-1	—
IC 4191 (a)*	2.40	Tsa04	5.52E-2	3.67E-2	5.42E-2	3.59E-2
IC 4191 (b)	2.40	Tsa04	6.85E-1	4.49E-2	6.71E-1	4.40E-2
IC 4406	1.90	Tsa04	6.30E-2	1.40E-2	6.44E-2	1.44E-2
IC 4593	3.60	Rob05	4.13E-1	5.76E-1	4.13E-1	5.76E-1
IC 4663	39.00	Moh23	—	—	4.94E-2	—
IC 4699	6.20	WL07	5.46E-2	—	5.57E-2	—
IC 4776	1.75	Sow17	—	—	6.86E-2	4.25E-2
IC 4846 (a)*	1.50	WL07	2.09E-1	2.22E-1	1.90E-1	2.02E-1
IC 4846 (b)	2.91	Wes05	8.27E-2	—	8.27E-2	—
IC 4997	4.87	RP22	—	—	9.00E-2	—
IC 5217	2.26	Wes05	—	—	—	—
K 648	2.99	Ots15A	5.29E-2	2.72E-2	5.36E-2	2.76E-2
M 1-20	1.40	WL07	2.40E-1	1.83E-1	2.47E-1	1.87E-1
M 1-25	1.80	Gar13	5.49E-2	—	1.31E-1	—
M 1-29	3.00	WL07	1.98E-1	1.14E-1	3.22E-1	1.85E-1
M 1-30	2.40	Gar13	3.24E-2	2.79E-2	1.06E-1	9.11E-2

Continue

Table A4 – Continued

Name	ADF	Ref. ADF	$M_{ion}(\text{[S II]})$ Slit (M_{\odot})	$M_{ion}(\text{[Cl III]})$ Slit (M_{\odot})	$M_{ion}(\text{[S II]})$ Global (M_{\odot})	$M_{ion}(\text{[Cl III]})$ Global (M_{\odot})
M 1-31	2.11	Gar18	3.07E-1	7.95E-2	1.010	2.61E-1
M 1-32	3.00	Gar13	4.71E-3	4.79E-3	1.48E-2	1.50E-2
M 1-33	2.77	Gar18	2.78E-1	1.94E-1	2.62E-1	1.83E-1
M 1-42 (a)*	20.00	Liu01	2.54E-1	1.59E-1	2.60E-1	1.63E-1
M 1-42 (b)	22.00	McN16	2.33E-1	1.66E-1	2.39E-1	1.70E-1
M 1-60	2.75	Gar18	2.46E-1	1.31E-1	2.07E-1	1.10E-1
M 1-61 (a)*	1.60	Gar13	6.84E-2	8.53E-2	1.04E-1	1.29E-1
M 1-61 (b)	2.00	WL07	7.80E-2	5.27E-2	8.36E-2	5.65E-2
M 1-73	3.61	Wes05	1.95E-1	—	1.95E-1	—
M 1-74	2.14	Wes05	1.84E-1	—	1.84E-1	—
M 2-4	1.90	WL07	2.93E-1	2.07E-1	3.69E-1	2.61E-1
M 2-6	2.30	WL07	7.62E-2	4.33E-1	1.63E-1	9.27E-1
M 2-23	1.40	WL07	1.13E-1	1.01E-1	1.16E-1	1.04E-1
M 2-24	17.00	Zha03	3.77E-1	—	3.86E-1	—
M 2-27	2.20	WL07	9.58E-2	4.11E-2	1.03E-1	4.40E-2
M 2-31	2.42	Gar18	1.62E-1	9.06E-2	1.79E-1	1.00E-1
M 2-33	2.20	WL07	2.75E-1	—	4.90E-1	—
M 2-36 (a)	5.00	Liu01	9.09E-2	5.60E-2	1.62E-1	9.98E-2
M 2-36 (b)*	6.76	Esp21	1.18E-1	7.27E-2	2.11E-1	1.30E-1
M 2-39	0.40	WL07	7.99E-2	1.99E-1	6.95E-2	1.73E-1
M 2-42	2.10	WL07	2.17E-1	1.85E-1	2.08E-1	1.77E-1
M 3-7	4.40	WL07	1.48E-1	2.27E-1	1.82E-1	2.79E-1
M 3-15	2.30	Gar13	6.20E-1	4.46E-1	2.44E-1	1.76E-1
M 3-21	2.60	WL07	7.45E-2	5.57E-2	6.96E-2	5.20E-2
M 3-27 (a)	5.48	Wes05	—	—	—	—
M 3-27 (b)*	3.26	RPB24	—	—	9.61E-1	—
M 3-29	2.20	WL07	1.60E-1	—	2.41E-1	—
M 3-32	17.80	WL07	1.48E-1	3.53E-1	1.33E-1	3.16E-1
M 3-33	6.60	WL07	2.41E-1	1.32E-1	2.06E-1	1.13E-1
M 3-34	4.23	Wes05	—	—	—	—
Me 2-2	2.10	Wes05	1.83	—	1.83	—
MPA J1759-3007	62.00	Wes18	—	—	—	—
MyCn 18	1.80	Tsa04	1.05E-1	4.20E-2	1.26E-1	5.05E-2
NGC 40	17.80	Liu04A	6.23E-1	1.07	3.19E-1	5.50E-1
NGC 1501	32.00	Erc04	—	—	1.16E-1	5.18E-2
NGC 2022	16.00	Tsa04	1.81E-1	8.28E-2	1.81E-1	8.28E-2
NGC 2392 (a)	1.65	Zha12	—	—	1.31E-1	2.09E-1
NGC 2392 (b)*	1.65	Zha12	—	—	4.76E-1	2.97E-1
NGC 2440	5.40	Tsa04	3.32E-2	—	3.32E-2	—
NGC 2867 (a)*	1.49	Gar09	—	—	1.27E-1	1.02E-1
NGC 2867 (b)	1.77	Gar09	—	—	1.96E-1	1.09E-1
NGC 3132	2.40	Tsa04	2.71E-1	1.65E-1	2.71E-1	1.65E-1
NGC 3242	2.20	Tsa04	3.20E-1	4.05E-1	3.20E-1	4.05E-1
NGC 3918 (a)	1.80	Tsa04	1.62E-1	1.19E-1	1.62E-1	1.19E-1
NGC 3918 (b)*	1.85	Gar15	5.84E-3	4.86E-3	9.61E-2	8.00E-2
NGC 5189	1.60	Gar13	1.81E-4	1.59E-4	4.67E-2	4.10E-2
NGC 5307	1.90	Rui03	1.01E-2	2.82E-2	5.64E-2	1.58E-1
NGC 5315 (a)*	1.58	Ma17	—	—	8.96E-2	2.85E-2
NGC 5315 (b)	2.00	Tsa04	1.13E-1	2.88E-2	1.13E-1	2.88E-2
NGC 5882	2.10	Tsa04	1.95E-1	2.06E-1	1.99E-1	2.10E-1
NGC 6153 (a)*	10.00	Liu00	—	—	2.30E-1	1.83E-1
NGC 6153 (b)	11.00	McN16	—	—	2.28E-1	—
NGC 6210 (a)	2.50	Rob05	—	—	—	—
NGC 6210 (b)*	3.10	Liu04A	1.92E-1	1.91E-1	1.92E-1	1.91E-1
NGC 6302	3.60	Tsa04	4.41E-2	1.67E-2	4.41E-2	1.67E-2
NGC 6326	23.00	Wes18	—	—	4.06E-1	—
NGC 6337	18.00	Wes18	—	—	1.59E-1	—
NGC 6369	1.40	Gar13	2.63E-3	2.44E-3	1.88E-1	1.74E-1
NGC 6439	6.20	WL07	2.74E-1	2.12E-1	3.08E-1	2.38E-1
NGC 6543 (a)	2.07	Rob05	—	—	—	—
NGC 6543 (b)	2.74	Rob05	—	—	—	—
NGC 6543S (c)*	3.00	Wes04	—	—	1.38E-1	1.44E-1
NGC 6565	1.70	WL07	1.44E-1	1.28E-1	1.55E-1	1.37E-1
NGC 6567	2.20	WL07	1.71E-1	6.24E-2	1.74E-1	6.35E-2

Continue

Table A4 – Continued

Name	ADF	Ref. ADF	$M_{ion}(\text{[S II]})$ Slit (M_\odot)	$M_{ion}(\text{[Cl III]})$ Slit (M_\odot)	$M_{ion}(\text{[S II]})$ Global (M_\odot)	$M_{ion}(\text{[Cl III]})$ Global (M_\odot)
NGC 6572 (a)	1.38	Rob05	—	—	—	—
NGC 6572 (b)	1.50	Tsa04	—	—	—	—
NGC 6572 (c)	1.54	Rob05	—	—	—	—
NGC 6572 (d)*	1.60	Liu04A	1.26E–1	4.74E–1	1.26E–1	4.74E–1
NGC 6620	3.20	WL07	1.35E–1	9.99E–2	1.35E–1	9.99E–2
NGC 6644	1.90	Tsa04	—	—	—	—
NGC 6720 (a)*	2.40	Liu04A	2.25E–1	1.86E–1	2.25E–1	1.86E–1
NGC 6720 (b)	5.00	Gar01	—	—	—	—
NGC 6741	1.90	Liu04A	2.06E–1	1.67E–1	2.15E–1	1.75E–1
NGC 6778	18.00	Jon16	2.67E–1	—	2.99E–1	—
NGC 6790 (a)	1.44	Rob05	—	—	—	—
NGC 6790 (b)*	1.70	Liu04A	1.01E–1	1.36E–1	1.01E–1	1.36E–1
NGC 6803	2.71	Wes05	2.35E–1	1.51E–1	2.35E–1	1.51E–1
NGC 6807	2.00	Wes05	1.81E–1	—	1.81E–1	—
NGC 6818	2.90	Tsa04	2.25E–1	1.36E–1	2.25E–1	1.36E–1
NGC 6826	1.90	Liu04A	1.61E–1	1.84E–1	1.54E–1	1.76E–1
NGC 6833	2.47	Wes05	—	—	—	—
NGC 6879	2.46	Wes05	—	—	—	—
NGC 6884	2.30	Liu04A	1.58E–1	1.76E–1	1.58E–1	1.76E–1
NGC 6891	1.52	Wes05	—	—	—	—
NGC 7009 (a)	5.00	Liu95	—	—	—	—
NGC 7009 (b)*	5.00	Fan11	—	—	1.50E–1	1.39E–1
NGC 7026	3.36	Wes05	—	2.48E–1	—	2.48E–1
NGC 7027 (a)	3.58	Rob05	—	—	—	—
NGC 7027 (b)*	1.30	Zha05	—	—	2.65E–2	2.54E–2
NGC 7662	2.00	Liu04A	2.90E–1	3.17E–1	2.90E–1	3.17E–1
Ou 5	56.00	Cor15	2.43E–2	—	—	—
PB 8	2.57	Gar09	—	—	1.29E–1	1.44E–1
PC 14	1.90	Gar13	1.97E–2	2.00E–2	7.25E–2	7.37E–2
Pe 1-1	1.70	Gar13	3.76E–2	2.19E–2	8.06E–2	4.69E–2
Pe 1-9	60.00	Wes18	—	—	8.09E–2	—
Sp 3	24.00	Mis19	—	—	6.29E–2	3.96E–2
Sp 4-1	2.94	Wes05	—	—	—	—
Vy 1-2 (a)*	5.34	RP22	9.17E–2	4.87E–2	9.17E–2	4.87E–2
Vy 1-2 (b)	6.17	Wes05	3.48E–1	—	3.48E–1	—
Vy 2-1	2.00	WL07	3.34E–1	1.76E–1	3.92E–1	2.06E–1
Vy 2-2 (a)*	4.30	RP22	3.82E–2	3.43E–3	3.82E–2	3.43E–3
Vy 2-2 (b)	11.80	Wes05	—	—	—	—
Wray 16-423	1.64	Ots15B	2.20E–1	1.23E–1	1.44E–1	8.06E–2

* Adopted mass and ADF values

References: Cor15: Corradi et al. (2015), Erc04: Ercolano et al. (2004), Esp21: Espíritu & Peimbert (2021), Fan11: Fang & Liu (2011), Gar09: García-Rojas et al. (2009), Gar13: García-Rojas et al. (2013), Gar15: García-Rojas et al. (2015), Gar18: García-Rojas et al. (2018), Jon15: Jones et al. (2015), Jon16: Jones et al. (2016), Liu00: Liu et al. (2000), Liu04A: Liu et al. (2004a), Liu06: Liu et al. (2006), Ma17: Madonna et al. (2017), McN16: McNabb et al. (2016), Mis19: Miszalski et al. (2019), Moh23: Mohery et al. (2023), Ots09: Otsuka et al. (2009), Ots10: Otsuka et al. (2010), Ots11: Otsuka et al. (2011), Ots13: Otsuka & Tajitsu (2013), Ots15A: Otsuka et al. (2015), Ots15B: Otsuka (2015), Ots17: Otsuka et al. (2017), Pen22: Peña et al. (2022), Rob05: Robertson-Tessi & Garnett (2005), Rui03: Ruiz et al. (2003), RP22: Ruiz-Escobedo & Peña (2022), RPB24: Ruiz-Escobedo et al. (2024), Sha04: Sharpee et al. (2004), Sim22: Simpson et al. (2022), Sow17: Sowicka et al. (2017), Tsa04: Tsamis et al. (2004), WL07: Wang & Liu (2007), Wes03: Wesson et al. (2003), Wes04: Wesson & Liu (2004), Wes05: Wesson et al. (2005), Wes18: Wesson et al. (2018), Zha05: Zhang et al. (2005), Zha12: Zhang et al. (2012).